

# Bitcoin's Crypto Flow Network

Yoshi FUJIWARA<sup>1</sup> and Rubaiyat ISLAM<sup>1</sup>

<sup>1</sup>*Graduate School of Information Science, University of Hyogo, Kobe 650-0047, Japan*

*E-mail: yoshi.fujiwara@gmail.com*

(Received May 31, 2021)

How crypto flows among Bitcoin users is an important question for understanding the structure and dynamics of the cryptoasset at a global scale. We compiled all the blockchain data of Bitcoin from its genesis to the year 2020, identified users from anonymous addresses of wallets, and constructed monthly snapshots of networks by focusing on regular users as big players. We apply the methods of bow-tie structure and Hodge decomposition in order to locate the users in the upstream, downstream, and core of the entire crypto flow. Additionally, we reveal principal components hidden in the flow by using non-negative matrix factorization, which we interpret as a probabilistic model. We show that the model is equivalent to a probabilistic latent semantic analysis in natural language processing, enabling us to estimate the number of such hidden components. Moreover, we find that the bow-tie structure and the principal components are quite stable among those big players. This study can be a solid basis on which one can further investigate the temporal change of crypto flow, entry and exit of big players, and so forth.

*Presented at the conference "Blockchain in Kyoto 2021", and forthcoming in the JPS Conference Proceedings.*

**KEYWORDS:** Bitcoin, cryptoasset, bow-tie structure, Hodge decomposition, non-negative matrix factorization, latent Dirichlet allocation, complex network

## 1. Introduction

Cryptoasset or cryptocurrency is essentially a digital ledger to record transactions between creditors and debtors, just like money. The digital system is based on a collection of non-centralized ledgers, called blockchain, which contains all the historical record of transactions among anonymous users. Today there are many cryptoassets being exchanged in markets with fiat currencies and also with each other. The market capitalization is so huge in total ranging from one to a few trillion USD, and highly volatile potentially having a big impact even on asset markets and prices of non-crypto at a global scale.

In this paper, we study Bitcoin, the largest one dominating nearly half of the market capitalization at the time of writing. We attempt to understand the flow of crypto as a complex network comprising of the users as nodes and the crypto flow as links. There are a number of studies from such a viewpoint of complex network on cryptoassets. See [1–16] for example, and references therein.

Specifically, in this paper, we focus on “big players” who are defined as persistently appearing users, likely to be involved in transactions of high frequencies and large amounts, and address the following questions. First, it is important to identify the users in the upstream, downstream, or core in the entire crypto flow. We shall examine the so-called “bow-tie” structure of the network of those big players to classify the location of the crypto flow based on the binary relationship of links. Second, we measure the location in a more quantitative way by using the information of flow along the links in the combinatorial method of Hodge decomposition. Third question is to extract “principal components” hidden in the entire crypto flow so as to uncover a certain number of latent factors or components.

Fourth, because the network is changing in time, what can one say about the stability of the crypto flow?

In Section 2, we describe our dataset of Bitcoin to identify the anonymous addresses representing wallets into users. Then we define regular users as big players and construct networks. In Section 3.1, we perform the bow-tie analysis to locate users in the stream of crypto flow. In Section 3.2, we use the method of Hodge decomposition to quantify the location of users. In Section 3.3, we introduce non-negative matrix factorization as a method of matrix decomposition to reveal principal components hidden in the flow. We shall show in Section 3.4 that the method can be interpreted as a probabilistic model, from which one can estimate the number of components. In Section 3.5, we find about a dozen of principal components among several hundred big players, and show that the temporal change of the network is quite stable. In Section 4, we discuss about several aspects, being worth further investigation, and conclude in Section 5. We add Appendix A for the identities (actual names, business, and so forth) of selected users. Appendix B illustrates the networks in adjacency matrices. Appendix C briefly summarizes the above mentioned probabilistic model in relation to latent Dirichlet allocation, from which the estimation on the number of components is done in Appendix D.

## 2. Data

We employ the dataset of all transactions recorded in the Bitcoin blockchain from the genesis block (first block issued on January 9, 2009) until the block of height 63,299 (inclusive; issued on June 4, 2020). Each transaction is a transfer of a certain amount of BTC (monetary unit of Bitcoin) from one or more addresses to others as we will see shortly. We call such a transfer of BTC as crypto flow. An address is something like a wallet possessed by a user who can be an individual or, more frequently today, an agent in the business of exchanges, services, gambling, and so forth.

In the dataset, total number of transactions was 1.38 billion, while the number of different addresses was about 657 million. To study crypto flow of Bitcoin, one needs to know users, rather than the addresses. However, it is not straightforward to identify users from addresses because of the very nature of anonymity inherent in the core technology of blockchain. See [17] for technical details.

Let us employ a simple but useful method to identify users from addresses to construct a giant graph comprising of nodes as users and edges as crypto flow. We shall see that more than 60% of the addresses can be identified with users. Additionally we will see that a number of users can be revealed with their actual names, types of business, and sometimes geographical location at a global scale. Then we define regular users as big players in order to focus on a subgraph comprising of frequently appearing users who are involved in crypto flow with huge amounts of BTC. The subgraph will be studied in the subsequent sections.

### 2.1 Identification of Users from Addresses

Consider an example of such a transaction (TX) that one day Alice transferred 1 BTC to Bob:

$$\text{TX}_1 : \{a_1, a_2\} \rightarrow \{a_{123}, a_1\}, \quad (1)$$

where the addresses  $a_1$  and  $a_2$  belong to Alice, while  $a_{123}$  belongs to Bob. Alice needs more than one address as input of  $\text{TX}_1$ , because a single one was not sufficient to fulfill the amount of 1 BTC. Output of  $\text{TX}_1$  includes  $a_1$  representing the change. Another day, Alice did another transaction:

$$\text{TX}_2 : \{a_1, a_3\} \rightarrow \{a_{45}, a_3\}, \quad (2)$$

where the address  $a_3$  also belongs to Alice. Obviously, multiple addresses, if and only if they appear in an input of a transaction, belong to the same user, namely her wallets. As a consequence from both of (1) and (2), it follows that  $a_1, a_2, a_3$  can be identified to belong to the same user. Note that  $a_2$  and

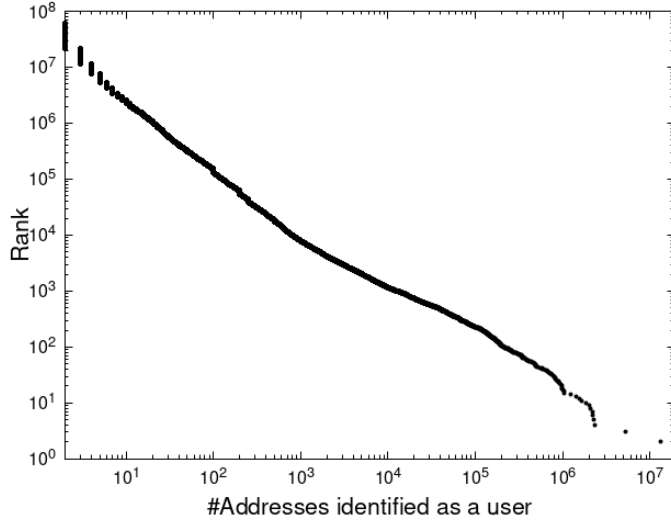


**Fig. 1.** Rank-size plot for the number of addresses identified with users. Size (horizontal) is the number of addresses identified with users of type A (a group of addresses appearing in multiple inputs of transactions, so identified as user; see main text). Rank (vertical) is the descending order of the size. Maximum size is nearly 20 million, while minimum is 2 and average is 6.7.

$a_3$  did not appear in any record of transactions,  $TX_1$  and  $TX_2$ . By looking at all the transaction in the history, one can identify many addresses with users.

This simple but useful method to identify users from addresses was proposed by [1] and has been extensively used in the literature (see [4, 5] and the data of [18, 19], for example). We implemented an efficient algorithm of this method to process the above mentioned 657 million addresses in the 1.375 billion transactions. We found that 402 million addresses (more than 60%) can be identified to obtain 60 million different users (denoted as *type A*). The rest of 255 million addresses, which never appeared as multiple inputs in any transactions, are regarded as different users (*type B*). This procedure results in 315 million users all together.

Fig. 1 shows a rank-size plot, in which the size is the number of addresses identified with users of type A, and the rank is its descending order. The minimum size is 2 by construction, while the average is 6.7. It is interesting to observe that the rank-size plot is highly skewed with the maximum size being nearly 20 million! We labeled all the users of type A in a sequential user ID corresponding to the rank (e.g. 0000012345), while users of type B is labeled with its address (e.g. 3CjmbuRA1LEWmLHiWoSWHcWuTEVPfU24P).

A bunch of transactions is packed into a block in the blockchain. Each block has a timestamp of its birth, which is UTC (Coordinated Universal Time) when the block was mined or born as an empty ledger to be filled with transactions. We associate the time with the transactions contained in the block. Each block is mined in a mean time of 20 minutes or longer, as is well known, so it should be understood that by time we mean a rough estimate on when the transaction was made within an accuracy of an hour or so. One can use this information of the timestamp to obtain the intra-day activities of users. Fig. 2 is a schematic diagram for typical three users, presumably located in Asia, Europe including Africa, and USA.

Moreover, with the help of laborious investigation by [19], it is possible to unravel the identity of users of type A with actual names, types of business, and sometimes geographical location for many users. Appendix A is the summary of the unraveled identity. Table A-1 gives the classification of business into exchanges, gambling, pools, services and others. Nearly one third in the list are exchanges. Table A-2 is the list of countries of those exchanges, where China, UK, and USA are

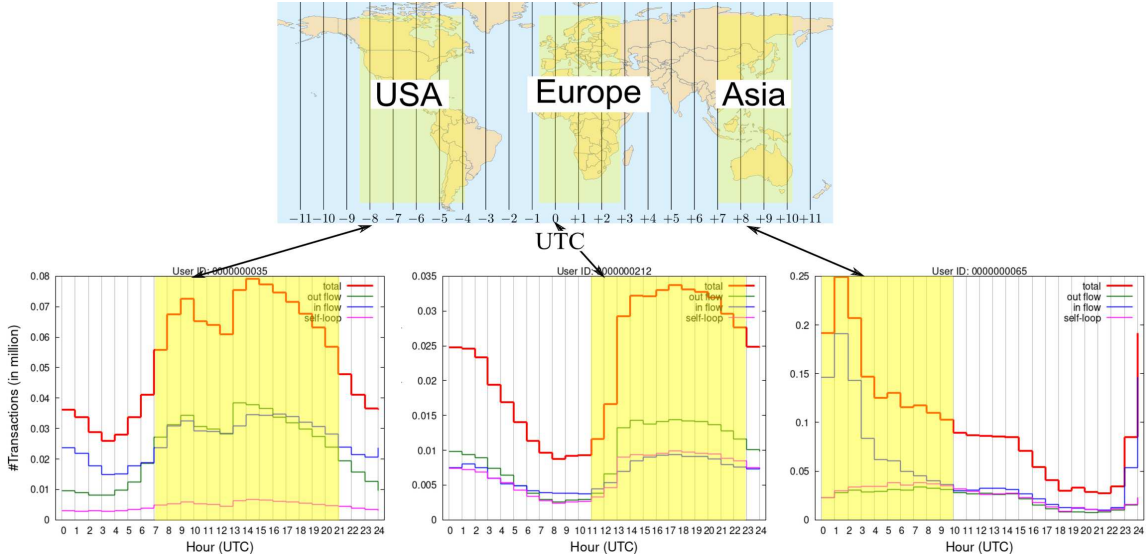


**Fig. 2.** Schematic diagram for the intra-day activities of users. Top is a world map with UTC (Coordinated Universal Time). The bottom three plots depict the number of transactions involving three users. Each plot shows the numbers of transactions of out-flow (green), in-flow (blue), self-loop (magenta), and their total (bold red), where each number is accumulated during the year 2019. Out-flow, in-flow, and self-loop are respectively the transaction in which the user is its source, destination, and both of them simultaneously. A peak of the red line shows the most active time, corresponding to the daytime of USA, Europe, and Asia (left to right). Arrows indicate noon of specific locations.

dominant, followed by Canada, Australia, Brazil, Singapore, and Russia. In fact, as found in the top of Table A-3, the user ID 0000000000 corresponding to the maximum size in Fig. 1 is actually Bit-x.com and Xapo.com, the former of which is an agent of exchange in South Africa.

Exchanges are a typical category of “big players” in the sense that they actually hold a huge number of individuals and agents as customers resulting in a large number of transfers. As a matter of fact, the daily number of transfers has an interesting weekly pattern. There is significantly less activity in weekends than in weekdays as found in recent data of Bitcoin<sup>1</sup> (see our previous study [21, 22]). Such a weekly pattern implies that those institutional agents are dominant in the entire flow of crypto.

## 2.2 Crypto Flow Network

Now all the transactions among addresses are converted into transfers from users to users, each of which has the following information:

- user of source  $s$ ,
- user of destination  $d$ ,
- amount of Bitcoin transferred from  $s$  to  $d$ , i.e.  $s \rightarrow d$ ,
- UTC time of transfer (from the block containing the transaction).

During a certain period of time  $T$ , for a pair of users, there can be more than one transfer as depicted in Fig. 3 (see the left-hand side). In this example, there are three transfer of crypto for  $i \rightarrow j$ , one for  $j \rightarrow i$ , and also two for  $i \rightarrow i$ . The last case of self-loop is possible, because one can receive a change in a transaction, and also because different addresses are possibly identified with a user, like

<sup>1</sup>Cryptoasset of XRP has a similar weekly pattern according to [20]. In the early history of Bitcoin, the weekly pattern was quite the opposite; more active in weekends, presumably because individuals were big players at that time.

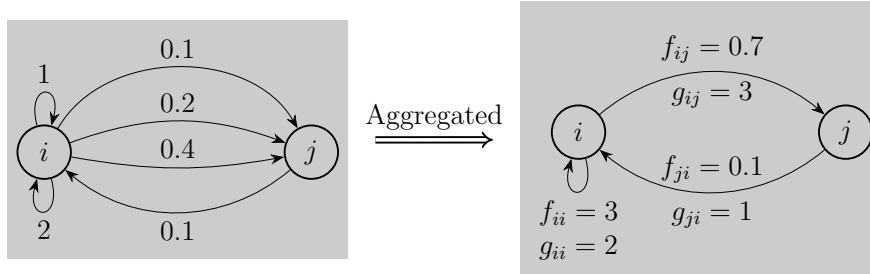


**Fig. 3.** Aggregation of transactions to construct crypto flow network. *Left:* During a given period of time, for a pair of users  $i$  and  $j$ , three transfers for  $i \rightarrow j$  with 0.1, 0.2, 0.4 in BTC, one of  $j \rightarrow i$  with 0.1, and two for  $i \rightarrow i$  with 1 and 2. *Right:* After aggregation, one has  $i \rightarrow j$  with frequency  $f_{ij} = 3$  and amount of flow  $g_{ij} = 0.7$ . Similarly,  $j \rightarrow i$  with  $f_{ji} = 1$  and amount of flow  $g_{ji} = 0.1$ , and  $i \rightarrow i$  with  $f_{ii} = 2$  and  $g_{ii} = 3$ .

an exchange. Given a time-scale  $T$ , it would be reasonable to aggregate these transactions as shown in the right-hand side of Fig. 3.

After the aggregation, one has a network comprising of nodes as users and edges with direction given by the transfer of crypto, frequency and amount of transfer occurred during the period of time. Let us denote the following variables which represent the strength or weight of each edge by

**frequency**  $f_{ij} \equiv$  frequency of transfers for  $i \rightarrow j$ ,

**amount of flow**  $g_{ij} \equiv$  amount of total transfers for  $i \rightarrow j$ .

Regarding the time-scale  $T$  for aggregating the transactions and the epoch to select in the historical data, we choose one month and the calendar year of 2019. By examining the time-series for the daily number and amount of transactions, we assumed that the period of one month is adequate to study the stability and temporal change of the crypto flow. Shorter period may lead to a trivial result for the stability and could be insufficient to detect the temporal change, if any change is present. Also longer period would be misleading due to non-equilibrium nature of the system. The year 2019 was chosen as the epoch, in which one does not see violent bubble or crush in the price.

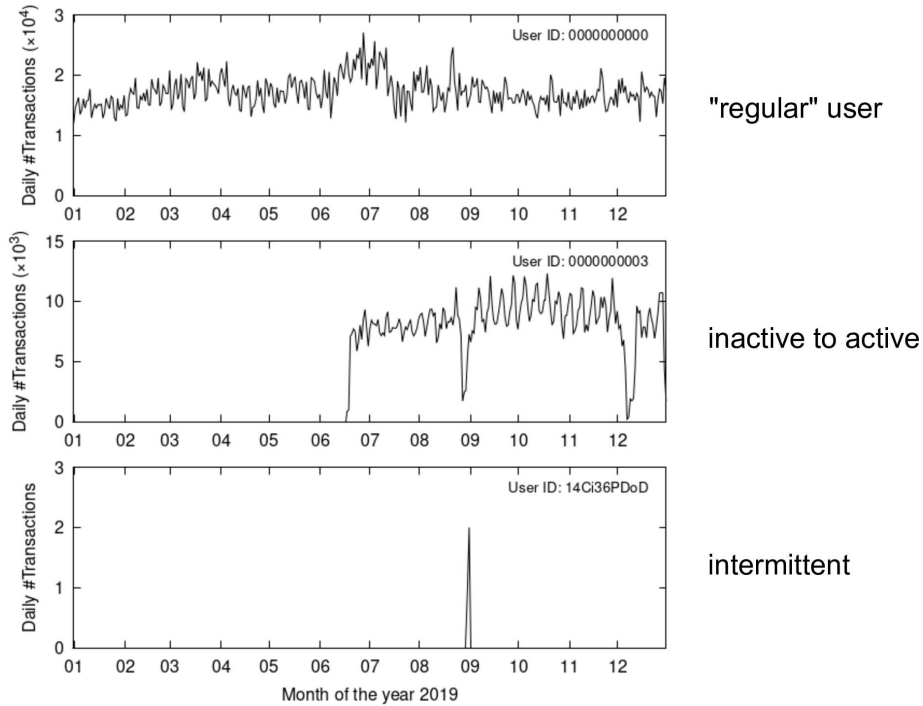
The number of all the users is huge, 315 million users in total. Fortunately, however, it is not necessary to include all of them, because most of them do not appear frequently. In the next section, we shall extract only a tiny part of the network by focusing on the “regular users” who appeared everyday during the specified period.

### 2.3 Regular Users as Big Players

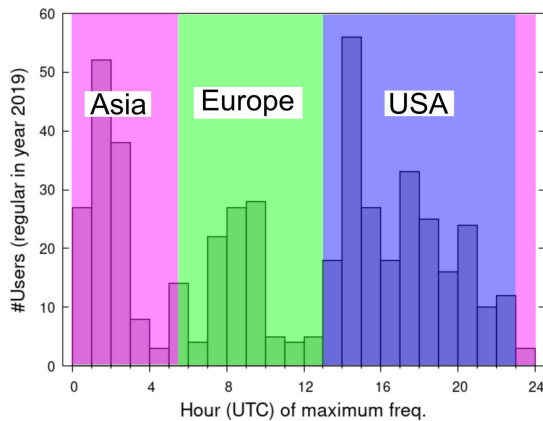
For our purpose in this paper, it is sufficient to focus on the crypto flow with high frequency and big amount of Bitcoin, because infrequent and/or small amount of flows is obviously unimportant for the understanding the entire flow. In other words, it suffices to focus on “big players” who are playing some dominant role in the game of crypto flow. It would be possible to define such a big player in different ways. In this study, we define it by looking at how persistently the user appears in transactions during our specified period of time.

Fig. 4 depicts examples of users who appear in different numbers of transactions on daily basis. The user of the top case is persistent in committing transactions with other users, which can be labeled as a “regular user”. The middle case changes the persistency from being inactive with no transaction with anyone else to being active in an abrupt way. The bottom case has little activity, just a few transactions on particular days having a strong intermittency.

We define *regular users* as those appearing everyday during the period of one year in 2019, and use them as big players. The number of regular users was 479. Then we construct a subgraph in each month, which is comprised of the regular users as nodes and the crypto flow as links, the latter of which are aggregated as described in Fig. 3. Thus we have 12 snapshots of such subgraphs, each



**Fig. 4.** Illustrative examples for the activities of users. Each plot depicts the daily number of transactions, in each of which the user is either source or destination of the transaction for the period of year 2019. Self-loops (case of the same source and destination) are excluded. Top is a “regular” user appearing every day. The middle user became active from being inactive, while the bottom one has intermittency in its activity. We focus on regular users in this paper.



**Fig. 5.** Activities of regular users, defined by each user’s peak of transactions, in UTC. Shaded region corresponds to the daytime of Asia, Europe, and USA (left to right).

corresponding to each month in the year, from January to December. Summarizing the processing of the whole dataset, we constructed the snapshots of networks denoted by  $G_t = (V_t, E_t)$ , where  $t$  is the month,  $V_t$  is the set of regular users,  $E_t$  is the set of links among them, each having the frequency and amount as depicted in Fig. 3.

We add Fig. 5 showing the histogram for the UTC time of highest activities of all the regular

users in the year of 2019. This information gives geographical locations of those regular users.

### 3. Analysis of Crypto Flow Network

#### 3.1 Basic Properties of Network

For each month  $t$ , we constructed a network denoted by  $G_t = (V_t, E_t)$  as described in the preceding section. Table I is the summary of basic properties of the networks in the year 2019.  $V_t$  corresponds to the regular users in each month, the number of which is shown by the column  $|V_t|$ . The column  $|E_t|$  is the number of edges, namely the number of different crypto flow from one user to another or to itself (self-loops as shown in parentheses). Most of the users have self-loops. Temporal change of the network causes the changes of  $V_t$  and  $E_t$ . The column of  $|V_t \cap V_{t+1}|$  is the number of users that are common to successive months in their appearance. One can see that most of the users are appearing successively. The same is true for the edges as shown in the column of  $|E_t \cap E_{t+1}|$ . In other words, the network is not changing drastically in terms of the entry and exit of nodes and edges during the time-scale of months.

**Table I.** Summary of basic properties of the networks in the year 2019, January to December.

$t$	$ V_t $	$ E_t $	$ V_t \cap V_{t+1} $	$ E_t \cap E_{t+1} $	GWCC	GSCC/IN/OUT/TE
01	470	17,215(408)	468	13,313	468(3)	327/24/113/4
02	470	16,658(407)	468	13,357	468(3)	322/20/120/6
03	473	17,618(408)	471	13,942	470(4)	327/25/113/5
04	473	17,691(415)	470	13,960	469(5)	336/16/115/2
05	472	17,903(416)	471	14,012	468(5)	330/23/112/3
06	471	17,787(412)	469	13,705	467(5)	318/23/124/2
07	472	17,292(410)	468	13,108	470(3)	333/21/110/6
08	468	16,534(402)	467	12,628	466(3)	321/18/123/4
09	470	16,288(407)	468	12,652	466(5)	325/23/113/5
10	469	16,317(402)	468	12,476	467(3)	322/21/119/5
11	470	15,859(409)	466	12,080	468(3)	324/23/116/5
12	466	15,584(390)	—	—	466(1)	323/18/120/5

Each column represents the following.

$t$ = month of the year 2019

$|V_t|$ = number of nodes

$|E_t|$ = number of edges (number of self-loops in parentheses)

$|V_t \cap V_{t+1}|$ = number of nodes common to successive months

$|E_t \cap E_{t+1}|$ = number of edges common to successive months

GWCC= number of nodes in giant weakly connected component (number of components in parentheses)

GSCC/IN/OUT/TE= number of nodes in giant strongly connected component/IN/OUT/tendrills

We found that most of the users have self-loops, as shown in the parentheses of column  $|E_t|$ , with the frequencies  $f_{ii}$  and the amounts  $g_{ii}$  being highly correlated with the number of addresses identified in the preceding Section 2.1 as naturally expected. Because our main interest in this paper is the crypto flow from one user to another, we remove all the self-loops in what follows.

Adjacent matrices with the strength of links given by the frequencies  $f_{ij}$  of  $G_t$  for all  $t$ 's are illustrated in Appendix B. One can see that the overall picture does not change in time, but the illustration does not help to uncover the nature of connectivity and flow.

To see the connectivity of network, namely how those regular users are linked among them and also how they are located in the stream of cypto flow, let us examine the property of connected com-

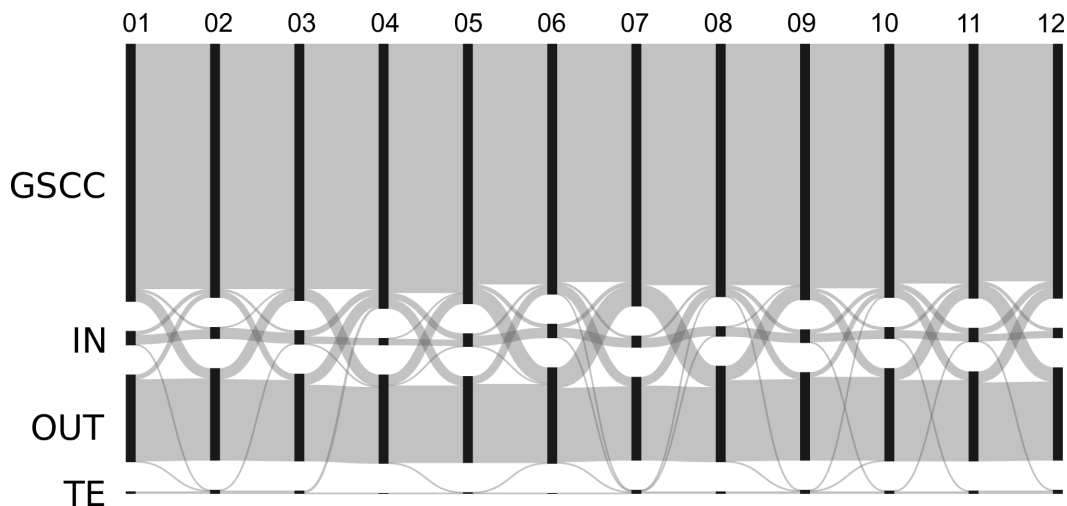


**Fig. 6.** Temporal change of bow-tie structure in an alluvial diagram. Monthly data of networks in the year 2019, January to December (from left to right). Vertical black segments in each month show the nodes of corresponding network grouped into GSCC (giant strongly connected component), IN, OUT, and TE (tendrils) in the bow-tie structure. Horizontal bands represent transitions among such groups from one month to its successive one.

ponents. First, decompose  $G_t$  into weakly connected components (WCC), i.e. connected components when regarded as an undirected graph. We found that there exists a giant WCC (GWCC) containing most of the users. See the column GWCC of Table I. There was only a small number of disconnected components as shown in the same column.

Then, in order to identify the location of users contained in the GWCC, we employed the well-known analysis of “bow-tie” structure [23]. In general, GWCC can be decomposed into the following parts:

**GSCC** Giant strongly connected component: the largest connected component when viewed as a directed graph. One or more directed paths exist for an arbitrary pair of firms in the component.

**IN** The nodes from which the GSCC is reached via at least one directed path.

**OUT** The nodes that are reachable from the GSCC via at least one directed path.

**TE** “Tendrils”; the rest of the GWCC.

It follows that

$$\text{GWCC} = \text{GSCC} + \text{IN} + \text{OUT} + \text{TE} \quad (3)$$

GSCC is the core of the crypto flow’s circulation. The IN and OUT parts are upstream and downstream of the flow respectively. The users in the part of IN are playing a role of suppliers of crypto, while the OUT users are considered to be consumers of crypto.

Table I shows the bow-tie structure in the column of GSCC/IN/OUT/TE. For example, in September, 470 users are located into GSCC (325 users), IN (23), OUT (113), and TE (5). One can observe that a large fraction of the users in the GWCC is located in the GSCC, as one can easily interpret this fact in the way that those regular users are circulating crypto globally. There are a less fraction of the users in IN and OUT with asymmetry in the numbers.

It would be interesting to see how the individual users are located in the temporal change of the network. Fig. 6 depicts such a diagram of temporal change from one month to its successive one in the whole year. One can see that the groups of GSCC, IN, and OUT are very stable in each membership of users. This fact means that those users appearing in successive months are playing stable roles in the crypto flow’s circulation and the location of upstream and downstream. We remark that analysis



of bow-tie structure is based on the binary links, namely either presence or absence among the nodes, but not on the strength of links such as frequency and amount of crypto flow. In the next section, we shall see how to quantify the location of users by using the so-called Hodge decomposition.

### 3.2 Hodge Decomposition

Helmholtz-Hodge-Kodaira decomposition, or simply Hodge decomposition, is a combinatorial method to decompose flow on a network into circulation and gradient flow. Original idea dates back to the Helmholtz theorem in vector analysis, which states that under appropriate conditions any vector field can be uniquely represented by the sum of an irrotational or rotation-free (curl-free) vector field and a divergence-free (solenoidal) vector field. The theorem can be generalized from Euclidean space to graph and other entity as shown by Hodge, Kodaira and others. See [24–26] for readable exposition. The method has a wide range of applications in the studies such as neural network [27], economic networks [28, 29], and also our previous work on Bitcoin and [30].

We recapitulate the method briefly for the present manuscript to be self-contained. Let  $A_{ij}$  denote the adjacency matrix:

$$A_{ij} = \begin{cases} 1 & \text{if there is a link of transfer from user } i \text{ to } j, \\ 0 & \text{otherwise.} \end{cases} \quad (4)$$

We excluded all the self-loops, implying that  $A_{ii} = 0$ . Each link has a flow, denoted by  $\tilde{F}_{ij}$ , either of the frequency,  $f_{ij}$ , or the amount,  $g_{ij}$ , of the transfer from  $i$  to  $j$  (see Fig. 3). Define

$$\tilde{F}_{ij} = \begin{cases} f_{ij} \text{ or } g_{ij} & \text{if } A_{ij} = 1, \\ 0 & \text{otherwise.} \end{cases} \quad (5)$$

Note that there can be a pair of users such that  $A_{ij} = A_{ji} = 1$  and  $\tilde{F}_{ij}, \tilde{F}_{ji} > 0$ .

Let us define a “net flow”  $F_{ij}$  by

$$F_{ij} = \tilde{F}_{ij} - \tilde{F}_{ji} \quad (6)$$

and a “net weight”  $w_{ij}$  by

$$w_{ij} = A_{ij} + A_{ji}. \quad (7)$$

Note that  $w_{ij}$  is symmetric, i.e.,  $w_{ij} = w_{ji}$ , and non-negative, i.e.,  $w_{ij} \geq 0$  for any pair of  $i$  and  $j$ <sup>2</sup>.

Hodge decomposition is given by

$$F_{ij} = F_{ij}^{(c)} + F_{ij}^{(g)}, \quad (8)$$

where the *circular flow*  $F_{ij}^{(c)}$  satisfies

$$\sum_j F_{ij}^{(c)} = 0, \quad (9)$$

which implies that the circular flow is divergence-free. The *gradient flow*  $F_{ij}^{(g)}$  can be expressed as

$$F_{ij}^{(g)} = w_{ij}(\phi_i - \phi_j). \quad (10)$$

Thus the weight  $w_{ij}$  serves to make the gradient flow possible only where a link exists. We refer to the quantity  $\phi_i$  as the *Hodge potential*. Large value of  $\phi_i$  implies that the user  $i$  is in the upstream of the entire network, while small values implies  $i$  is in the downstream.

---

<sup>2</sup>It is remarked that (7) is simply a convention to consider the effect of mutual links between  $i$  and  $j$ . One could multiply (7) by 0.5 or an arbitrary positive number, which does not change the result significantly for a large network.

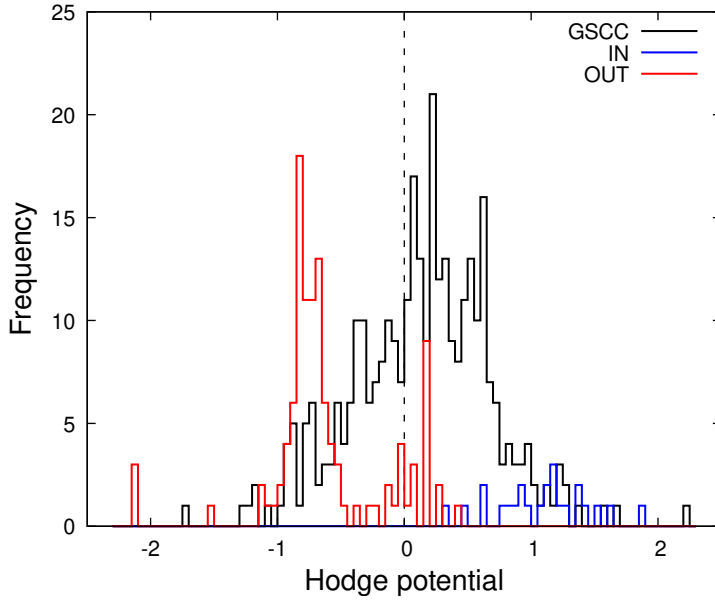


**Fig. 7.** Distributions for Hodge potentials of the users in GSCC (black), IN (blue), and OUT (red). The average of all the potential values is set to be zero (vertical dotted line). Data: 2019-09.

Combine (8), (9), and (10), one can derive the following equation to determine  $\phi_i$ .

$$\sum_j L_{ij}\phi_j = \sum_j F_{ij}, \quad (11)$$

for  $i = 1, \dots, N$ . Here,  $L_{ij}$  is the so-called graph Laplacian and defined by

$$L_{ij} = \delta_{ij} \sum_k w_{ik} - w_{ij}, \quad (12)$$

where  $\delta_{ij}$  is the Kronecker delta.

It is easy to show that the matrix  $L = (L_{ij})$  has only one zero mode (eigenvector with zero eigenvalue). The presence of this zero mode simply corresponds to the arbitrariness in the origin of  $\phi$ . All the other eigenvalues are positive (see, e.g., [30]). Therefore, (11) can be solved for the potentials by fixing the potentials' origin. We assume that the average value of  $\phi$  is zero.

Fig. 7 depicts the distributions for Hodge potentials of the users in GSCC, IN, and OUT. One can see that the entire set of distributions is bimodal having two peaks at positive and negative values, while there are a number of values around zero. Obviously, they correspond to IN, OUT, and GSCC, each being located in the upstream, downstream, and core of the entire crypto flow. Moreover, there exists a correlation between the value of the Hodge potential and the net amount of demand or supply of crypto by each user. See [30] for details, where we studied a daily snapshot of the network including all the users, not only big players. We claim that the same property holds also for the monthly data restricted to big players of regular users.

### 3.3 Non-negative Matrix Factorization

It would be a natural question whether there are distinctive ingredients of flows in the crypto flow or not. The analysis of bow-tie structure is based merely on the binary relationship of links, so does not give such information, because the crypto flows from upstream to downstream with circulation in the giant strongly connected component that occupies a large fraction of the entire network. In other

words, are there any “principal components” that constitute the entire flow in a decomposition? In order to find such principal components or latent factors in the transfer of crypto among big players, we shall apply *non-negative matrix factorization* (NMF) to the strength of links, namely the matrix of the frequencies and amounts of transfer. We recapitulate the method here. See [31–33] and references therein for introduction.

Let  $X$  be an  $N \times M$  non-negative matrix, in general, to start with; that is, its elements are all non-negative, denoted as  $X \geq 0$ . NMF gives an approximation of  $X$  by a product of two matrices:

$$X \approx SD, \quad (13)$$

where  $S, D$  are  $N \times K$  and  $K \times M$  non-negative matrices,  $S, D \geq 0$ , respectively<sup>3</sup>. In practice, one expects that  $K$  is much smaller than  $N$  and  $M$  so that the factorization gives a compact representation of  $X$ . We shall assume that  $N = M$  for our application of crypto flow among  $N$  users in what follows.

Explicitly in components, (13) reads

$$X_{sd} \approx \sum_{k=1}^K S_{sk} D_{kd}, \quad (14)$$

where the indices  $s$  and  $d$  represent source and destination ( $s, d = 1, \dots, N$ ) respectively, and  $X_{sd}$  is the strength of crypto flow, quantified by frequency  $f_{sd}$ , amount  $g_{sd}$ , or similar variables, from  $s$  to  $d$  in a certain period of time. We choose

$$X_{sd} = f_{sd}, \quad (15)$$

in this paper. See Fig. B-1 in Appendix B for the illustration of  $X_{sd}$ . We would expect that  $K \ll N$ , because of the sparsity of  $X$ . How to determine  $K$  is discussed later.

The approximation in (13) is actually given by the following optimization:

$$\min_{S, D \geq 0} F(X, SD), \quad (16)$$

where the function  $F(\cdot, \cdot)$  is the so-called Kullback-Leibler (KL) divergence defined by

$$F(A, B) = \text{KL}(A||B) \equiv \sum_{i,j} \left( A_{ij} \log \frac{A_{ij}}{B_{ij}} - A_{ij} + B_{ij} \right). \quad (17)$$

Note that  $F(A, B) = 0$  if and only if  $A = B$ . The reason why we choose the particular function of (17) will be clarified later<sup>4</sup>. Technically, one can solve (16) iteratively with the initialization of  $S, D$  using non-negative double singular value decomposition (see the review [32] and references therein). Although the iterative algorithm yields local minima, our numerical solutions under different random seeds gave essentially the same decomposition.

To understand the meaning of the decomposition, let us consider how a source distributes flow to different destinations. For an arbitrary source  $s$ , (14) can be written as

$$\mathbf{X}_s \approx \sum_{k=1}^K S_{sk} \mathbf{D}_k, \quad (18)$$

where  $\mathbf{X}_s$  is the vector of  $s$ -th row of  $X$ , and  $\mathbf{D}_k$  is the vector of  $k$ -th row of  $D$ . Equation (18) means that the flow from the source  $s$  can be expanded in terms of “basis” vectors,  $\mathbf{D}_k$  ( $k = 1, \dots, K$ ). The

<sup>3</sup>The decomposition is not unique due to trivial degrees of freedom. One is permutation,  $SD = S\pi\pi^{-1}D$ , where  $\pi$  is a permutation matrix simply exchanging indices. Another is scale transformation,  $SD = S\sigma\sigma^{-1}D$ , where  $\sigma$  is a diagonal matrix with all elements positive. We shall see that these degrees are fixed after appropriate normalization and ordering.

<sup>4</sup>See Section 3.4 for a probabilistic interpretation of choosing the KL divergence. Another functional form, often used, is the so-called Frobenius norm:  $F(A, B) = (1/2) \sum_{i,j} (A_{ij} - B_{ij})^2$ , which leads to a different probabilistic model.

components  $(\mathbf{D}_k)_d = D_{kd}$  represent how *destinations* are distributed among users in the  $k$ -th NMF component. It is convenient to normalize  $\mathbf{D}_k$  by L1-norm, that is, by defining

$$\tilde{D}_{kd} \equiv \frac{D_{kd}}{D_k} \quad \text{where} \quad D_k \equiv \sum_d D_{kd}, \quad (19)$$

so that one has

$$\sum_d \tilde{D}_{kd} = 1, \quad (20)$$

for all  $k$ . With respect to this normalized basis vectors, the expansion in (18) is rewritten as

$$\mathbf{X}_s \approx \sum_{k=1}^K (S_{sk} D_k) \tilde{\mathbf{D}}_k \quad \text{where} \quad (\tilde{\mathbf{D}}_k)_d = \tilde{D}_{kd}, \quad (21)$$

Thus the outgoing flow from the source  $s$  is approximately expressed by a linear combination of  $K$  normalized basis vectors  $\tilde{\mathbf{D}}_k$  with coefficients given by  $S_{sk} D_k$ .

Similarly, consider how a destination  $d$  collects flow from different sources. For an arbitrary destination  $d$ , (14) reads

$$\mathbf{X}_d \approx \sum_{k=1}^K D_{kd} \mathbf{S}_k, \quad (22)$$

where  $\mathbf{X}_d$  is the vector of  $d$ -th column of  $X$ , and  $\mathbf{S}_k$  is the vector of  $k$ -th column of  $S$ . The components of  $(\mathbf{S}_k)_s = S_{sk}$  represent how *sources* are distributed among users in this  $k$ -th NMF component. Define

$$\tilde{S}_{sk} \equiv \frac{S_{sk}}{S_k} \quad \text{where} \quad S_k \equiv \sum_s S_{sk}, \quad (23)$$

and one has

$$\sum_s \tilde{S}_{sk} = 1, \quad (24)$$

for all  $k$ . Then (22) is rewritten as

$$\mathbf{X}_d \approx \sum_{k=1}^K (D_{kd} S_k) \tilde{\mathbf{S}}_k \quad \text{where} \quad (\tilde{\mathbf{S}}_k)_s = \tilde{S}_{sk}. \quad (25)$$

Thus the incoming flow to the destination  $d$  is approximately expressed by a linear combination of  $K$  normalized basis vectors  $\tilde{\mathbf{S}}_k$  with coefficients given by  $D_{kd} S_k$ .

How can one determine  $K$ ? Obviously, the larger  $K$  is, the better the approximation (13) is, but with less parsimonious representation of the data. In the next section, let us make a detour to examine this issue from a different perspective.

### 3.4 NMF as a probabilistic model

We can interpret the NMF as a probabilistic model. Denote the right-hand of (14) by

$$\xi_{sd} \equiv \sum_k S_{sk} D_{kd}, \quad (26)$$

which are regarded as parameters to be estimated from the data  $X$  such that  $X_{sd}$  is assumed to be a random number chosen from a Poisson distribution with the parameter  $\xi_{sd}$  as

$$P(x|\xi) = e^{-\xi} \frac{\xi^x}{x!}. \quad (27)$$

It is easy to see that the log likelihood function  $L(\xi_{sd}) \equiv \log P(X_{sd} | \xi_{sd})$  takes the maximum value at  $\xi_{sd} = X_{sd}$ . Then one can introduce a quantity to measure how much the estimation of the parameters is good, that is

$$\sum_{s,d} (L(X_{sd}) - L(\xi_{sd})) = \sum_{s,d} \left( X_{sd} \log \frac{X_{sd}}{\xi_{sd}} - X_{sd} + \xi_{sd} \right), \quad (28)$$

to be *minimized*. One can see that this quantity is equivalent to the KL divergence in (17)<sup>5</sup>.

To express the entire framework in probabilistic terms more explicitly, let us normalize the data  $X$  in (15) by

$$\tilde{X}_{sd} = \frac{X_{sd}}{\sum_{s',d'} X_{s'd'}}. \quad (29)$$

Then let us rewrite (14) as

$$\tilde{X}_{sd} \approx \sum_k r_k \tilde{S}_{sk} \tilde{D}_{kd}, \quad (30)$$

where  $\tilde{D}_{kd}$  and  $\tilde{S}_{sk}$  were given by (19) and (23) respectively, and

$$r_k \equiv \frac{S_k D_k}{\sum_{k'} S_{k'} D_{k'}}, \quad (31)$$

which satisfies that  $\sum_k r_k = 1$ . Let us denote the right-hand side of (30) by

$$p_{sd} \equiv \sum_k r_k \tilde{S}_{sk} \tilde{D}_{kd}, \quad (32)$$

which satisfies that  $\sum_{s,d} p_{sd} = 1$ . We remark that the normalized weight  $r_k$  defined by (31) gives the information of relative importance of the  $k$ -th NMF component in the expansion with normalized basis vectors in (32). One can determine the ordering of NMF components uniquely according to the magnitudes of  $r_k$ .

Suppose that there are  $N_f$  transfers in total during a period of time. For each pair of source and destination,  $s$  and  $d$ , generate a transfer  $s \rightarrow d$  with the probability given by  $p_{sd}$ , being independently of other pairs. Under the assumption of a small probability of  $p_{sd}$  and a large number of  $N_f$ ,  $X_{sd}$  follows a Poisson distribution with the parameter,  $\xi_{sd} = N_f p_{sd}$ .

It turns out that the decomposition in (26), or equivalently (32), has an interesting connection with machine learning. In natural language processing, it is often necessary to extract *topics* among documents comprising of words or terms. In a situation of unsupervised learning, the task is to infer topics as hidden or latent variables, which can explain a collection of documents, each being an unordered set of terms. Probabilistic latent semantic analysis (PLSA) is a probabilistic model for doing such a task [36]. Suppose that there are  $N$  documents and  $M$  terms. Then the occurrence of terms can be expressed by a document-term matrix  $X$  with size  $N \times M$ , each element of which is the frequency of occurrence of a term in a document. Topics are latent variables to explain the data  $X$ . A topic is actually a probability distribution for the occurrence of terms with different probabilities. A document can have a mixture of topics. An example is a document on ‘‘influence of hosting Olympics to economy’’ with a mixture of topics on sports and economy.

One of the widely used model of PLSA is latent Dirichlet allocation (LDA). See Appendix C and references therein. For our purpose, it suffices to understand how terms are generated at locations of documents in a probabilistic way. The probability that a term is chosen at a location in a document is given by the sum of  $K$  factors, each of which is the product of two probabilities; the probability that

---

<sup>5</sup>We became aware that this argument is known in the literature. If one assumes Gaussian instead of Poisson, one would have Frobenius norm for KL divergence in (17). See [34]. One of the present authors (YF) learned a hint on the argument from Itsuki Noda in his application of NMF to transportation data [35].

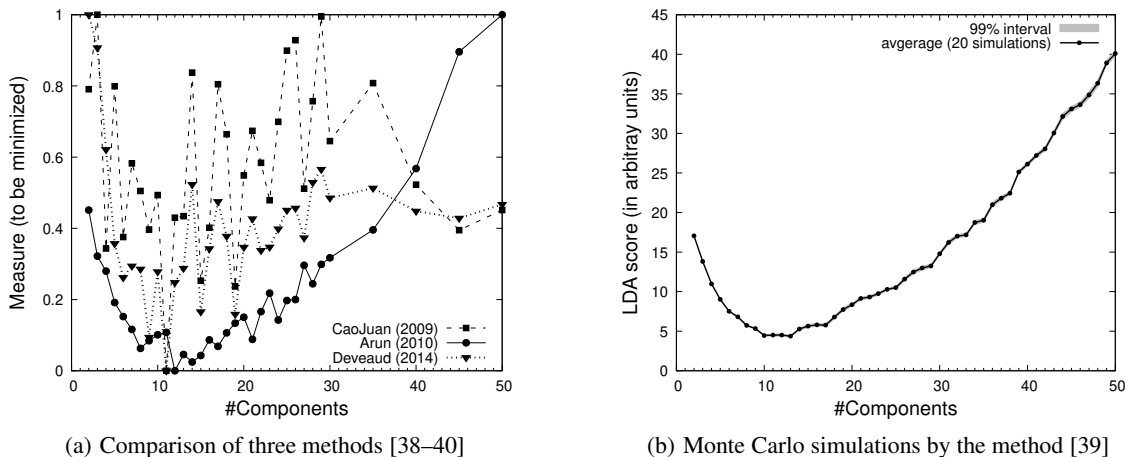


**Fig. 8.** Determining  $K$ , the number of NMF components, by using the concept of coherence in LDA. (a) Different methods [38–40] are compared. Each measure of coherence is drawn in the vertical axis so that it is to be minimized to find the optimal number of components. Maximum and minimum values in the region of  $K$  are scaled to 1 and 0 respectively to make the comparison easier. One can see that  $K = 11 \sim 13$  are optimal. (b) Monte Carlo simulations by the method [39] with 20 runs for each  $K$ . Averages (points) and 99% level (gray band, narrow) calculated from standard errors are drawn. We conclude that  $K = 13$  is optimal from this result (b).

a topic is selected in the document and the one that the term is chosen under the selected topic. See the equation of (C·11) in Appendix C. One can immediately see that (C·11) is essentially the same as (26), or equivalently (32).

Thus the matrix decomposition of NMF can be put in the framework of probabilistic model of PLSA and LDA. As a bonus, one can adopt the method of estimating the number of topics to our problem of determining the number of NMF components, denoted by  $K$  in both cases. Interested readers are guided to look at the literature [37–40] and others given at the end of Appendix C. Let us take a look at our results in the next section finishing the detour of this section.

### 3.5 Result of NMF for Crypto Flow

We first show a few results for a snapshot of September in the year 2019 (denoted as 2019-09), in order to verify if the idea in the preceding section works to determine the number of NMF components. Fig. 8 shows the measures of coherence by employing three different methods of LDA [38–40]. The methods give mostly the same optimal values of  $K$ , namely  $K = 11 \sim 13$ , consistently as shown in Fig. 8 (a). We found that the measure given in [39] is relatively stable and potentially useful to determine a specific value of  $K$ . So we performed Monte Carlo simulations in Fig. 8 (b), and were able to determine the optimal value as  $K = 13$ . For this data,  $X$  has the dimension of  $N = 470$ , so we conclude that one can have a small number of NMF components that can explain the entire flow among those regular users.

In Appendix D, we summarize the same result for the data in all the other months of the year 2019. We found that the optimal number  $K$  is quite small in the range more than 10 and less than 20, much smaller than the number of users,  $N \sim 500$  (see Table I). Additionally,  $K$  is relatively stable irrespectively of the temporal change. See Table D·1 and Fig. D·1.

Let us examine each NMF components obtained with the optimal value of  $K$ . Fig. 9 and Fig. 10 show the NMF components in terms of the basis vectors,  $\tilde{D}_k$  and  $\tilde{S}_k$ , respectively for  $k = 1, \dots, K$ . In Fig. 9, each plot shows the vector components of  $(\tilde{D}_k)_d = D_{kd}$  meaning how destinations are distributed among users  $d$  in the  $k$ -th NMF component. Similarly in Fig. 10, each plot shows the

vector components of  $(\widetilde{S}_k)_s = S_{sk}$  meaning how sources are distributed among users  $s$  in the  $k$ -th NMF component. See (19) and (23), and also note the normalization therein. Note that in each of Fig. 9 and Fig. 10, the plots are ordered (from top to bottom) in the descending order of the probability  $r_k$  given in (31).

One can immediately notice from the figures that the components of these basis vectors are concentrated on a limited number of users, but are not distributed among many users. To quantify the effective number of the concentration, let us use the inverse Herfindahl-Hirschman index, abbreviated as IHH, which is defined as follows. Consider “shares”  $x_i \geq 0$  among  $i = 1, \dots, N$  things with the sum equal to 1, i.e.  $\sum_i x_i = 1$ . The IHH is defined by

$$\text{IHH} \equiv \left( \sum_{i=1}^N x_i^2 \right)^{-1}. \quad (33)$$

When the shares are equal,  $x_i = 1/N$  for all  $i$ , then  $\text{IHH} = N$ . On the other hand, when there is the strongest concentration, namely,  $x_i = 1$  for a particular  $i$  and  $x_i = 0$  otherwise, then  $\text{IHH} = 1$ . So IHH can give an estimate of the effective number of large shares<sup>6</sup>. The idea can be applied to the basis vectors, because the vectors are normalized in the same way as shares. In Fig. 9 and Fig. 10, we displayed all the calculated IHH’s. One can see that the IHH’s are quite small ranging from a few to a dozen or so, compared with the total number of users  $N = 470$  for the data 2019-09 (see Table I).

How can we use the NMF components to understand the crypto flow? Choose a particular user  $s$  as a source  $s$ . The flow from  $s$  was approximately expressed by a linear combination of  $K$  normalized basis vectors  $\widetilde{D}_k$ , each depicted in Fig. 9, with the coefficients given in (21), i.e.  $S_{sk}D_k$ . The coefficients represent the strength of the decomposed flow from the source  $s$ . A similar argument holds by choosing a particular user  $d$  as a destination. The flow to  $d$  was expressed by a linear combination in (25) with the coefficients,  $D_{kd}S_k$ .

For example, consider the user with ID `00000000000` that is located in the GSCC, as a source  $s$ . Fig. 11 shows the coefficients corresponding to  $K$  components; see (a). One can see that the coefficients are non-zero at only four components. Such a sparseness tells that the flow from this user can be expressed with a few components. And the corresponding components have non-zero values at a small number (recall the IHH’s) of the vector components,  $D_{kd}$ , as shown in Fig. 9, implying that the users corresponding to these non-zero components constitute a cluster for the outgoing flow from the source  $s$ .

The same user `00000000000` can be regarded as a destination  $d$  in the GSCC. Fig. 11 (b) shows the coefficients, again non-zeros at only one or two components. Together with Fig. 10, one can find another cluster composed of a small number of users for the incoming flow to the  $d$ . Similar arguments hold for the users `00000006178` and `00000000012`, respectively located in the IN and OUT. See Fig. 11 (c) and (d). In this way, one can find clusters for either of or both of the outgoing and incoming flows of each user.

Each NMF component can be represented by a matrix, because the non-negative matrix of  $X_{sd}$  or its probabilistic counter part  $p_{sd}$  can be expressed by (18) or (32). It is possible to depict each component  $k$  by the matrix of  $S_{sk}\widetilde{D}_{kd}$  in the normalized way. Fig. 12 and Fig. 13 illustrate such matrices for the data of 2019-09. This should be compared with  $X_{sd}$  in Appendix B. One can see that the NMF components provide sparse matrices.

Finally, we find that the NMF components are relatively stable in the temporal change of network. Fig. 14 (a) shows the result for cosine similarities of the NMF basis vectors  $\widetilde{D}_k$  for the two successive months of 2019-09 and 2019-10. Fig. 14 (b) shows the result for  $S_k$  for the same data. In either of these results, one can see that the NMF components are quite similar except only a few permutation of indices.

---

<sup>6</sup>It is remarked that the paper [20] in this volume also applied but modifies Herfindahl-Hirschman index in an interesting way to characterize the frequencies of transactions in XRP.

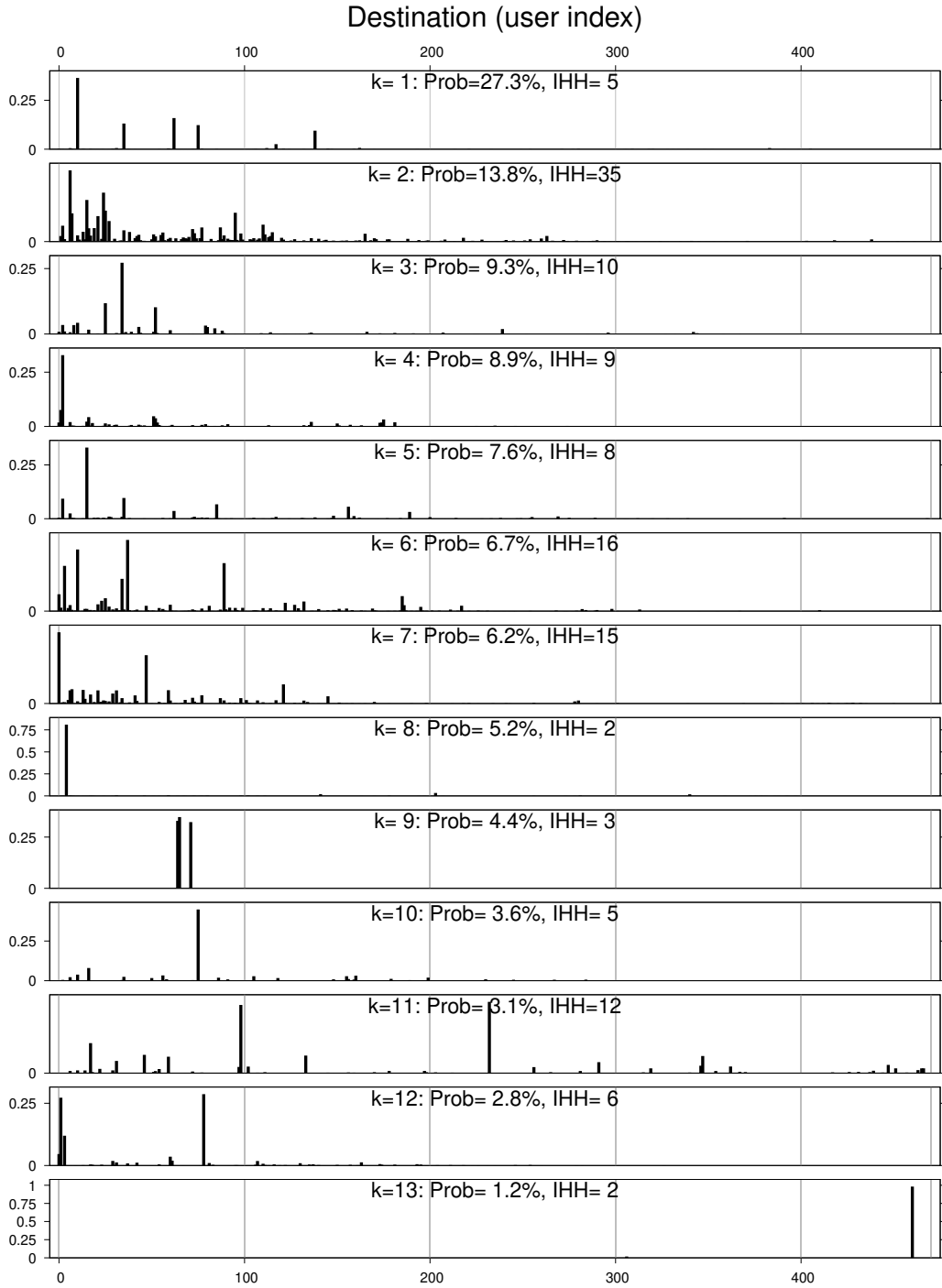


**Fig. 9.** NMF components  $\tilde{D}_k$  ( $k = 1, \dots, 13$ ) from top to bottom. Each plot  $(\tilde{D}_k)_d = D_{kd}$  shows how destinations are distributed among users  $d$  in the  $k$ -th NMF component. Note that  $\tilde{D}_k$  is normalized, i.e.  $\sum_d D_{kd} = 1$  for all  $k$ . See (19) and (20) in the main text. Also shown in each plot are the probability of the component, denoted by “Prob”, and the inverse Herfindahl-Hirschman index “IHH” representing the effective number of dominant users in the component. Data: 2019-09.



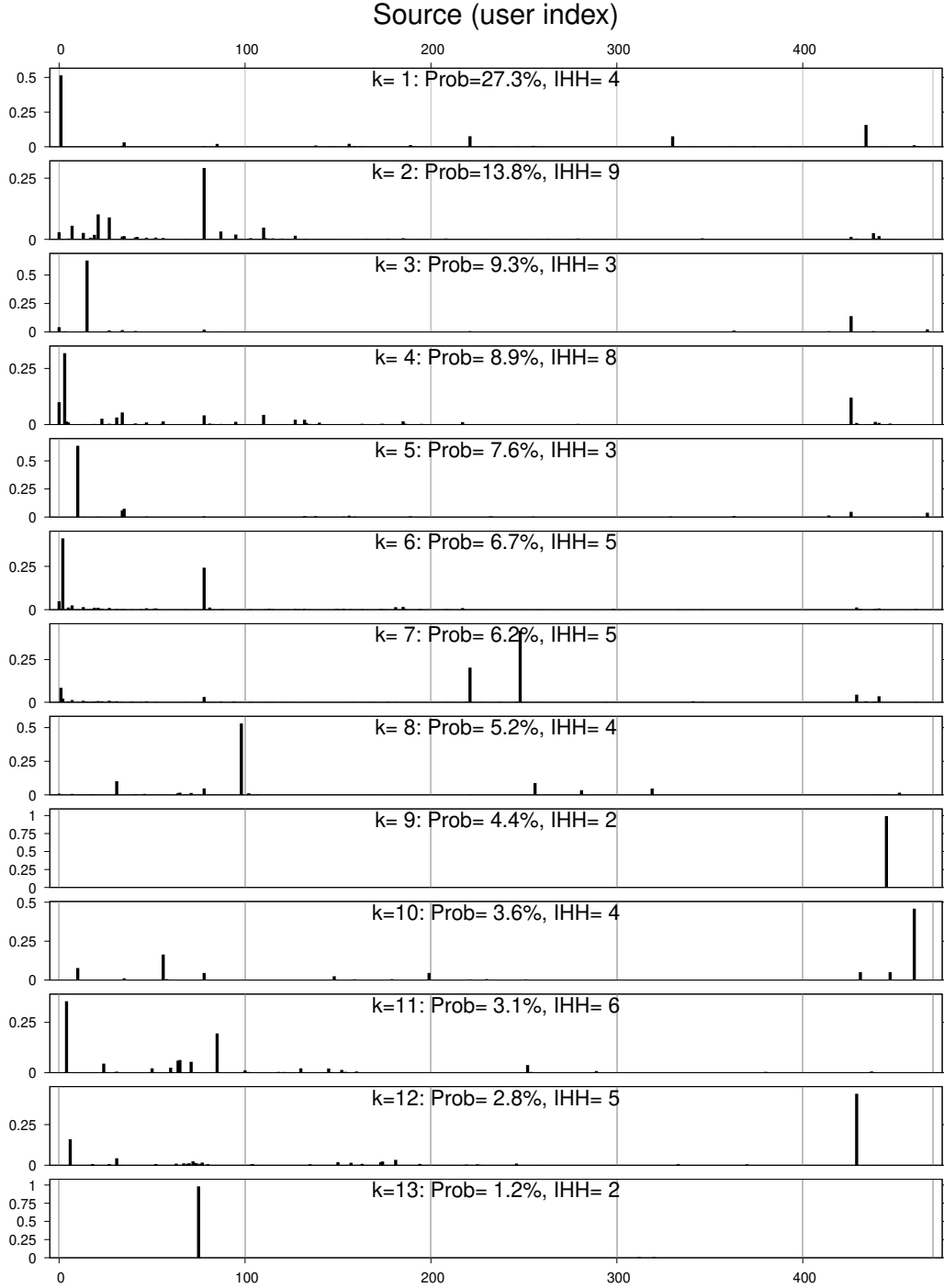


**Fig. 10.** NMF components  $\tilde{S}_k$  ( $k = 1, \dots, 13$ ) from top to bottom. Each plot  $(\tilde{S}_k)_s = S_{sk}$  shows how sources are distributed among users  $s$  in the  $k$ -th NMF component. Note that  $\tilde{S}_k$  is normalized, i.e.  $\sum_s S_{sk} = 1$  for all  $k$ . See (23) and (24) in the main text. See the caption of Fig. 9 for “Prob” and “IHH” in each plot. Data: 2019-09.

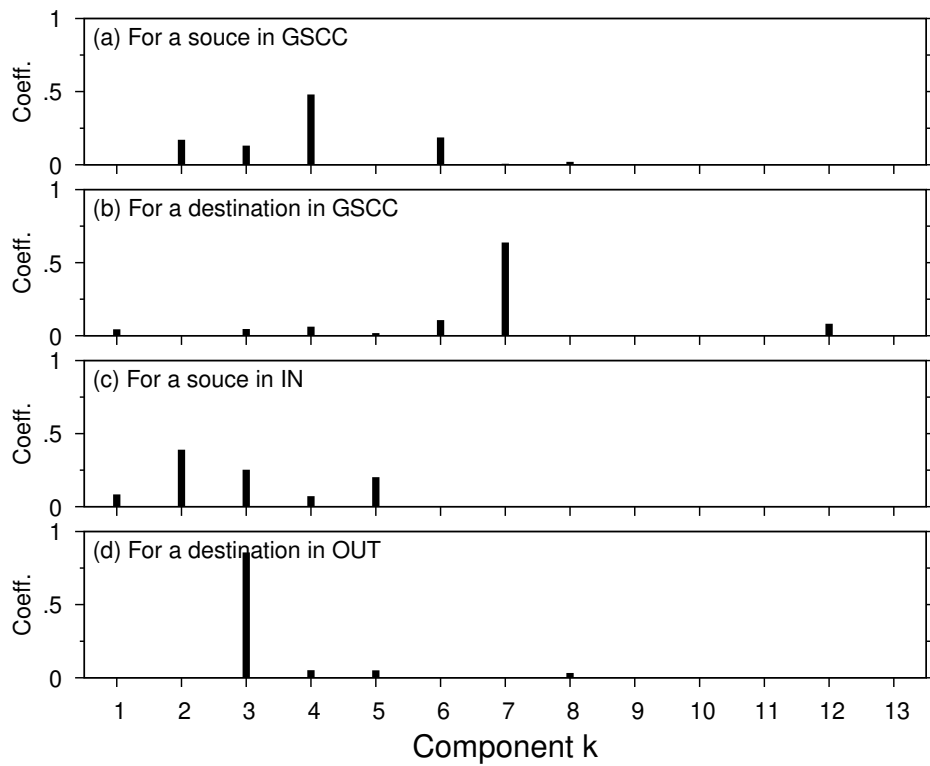


**Fig. 11.** Coefficients, with which crypto flow from or to a selected user is expanded with respect to the NMF components. The selected users are `0000000000` (a,b) included in the GSCC of bow-tie structure, `0000006178` (c) in the IN, and `0000000012` (d) in the OUT. The user `0000000000` can be source (a) and destination (b). The user of (c) is a source, and the user of (d) is a destination. The expansion is given by (21) for the selected source  $s$ , and by (25) for the selected destination  $d$ . Data: 2019-09.

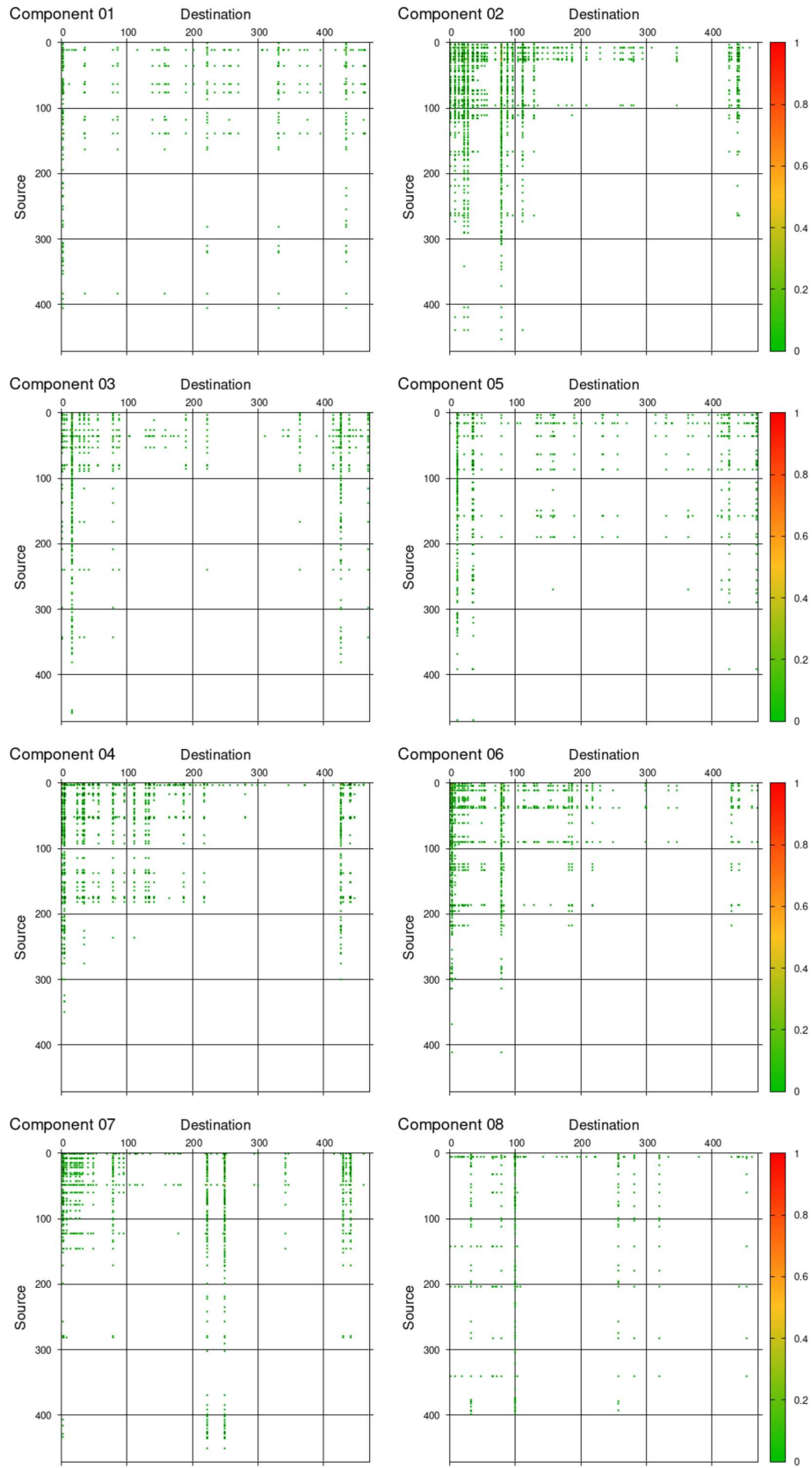


**Fig. 12.** NMF components  $k = 1, \dots, 8$  as matrices defined by  $\tilde{S}_{sk}\tilde{D}_{kd}$  in (32). Data: 2019-09.

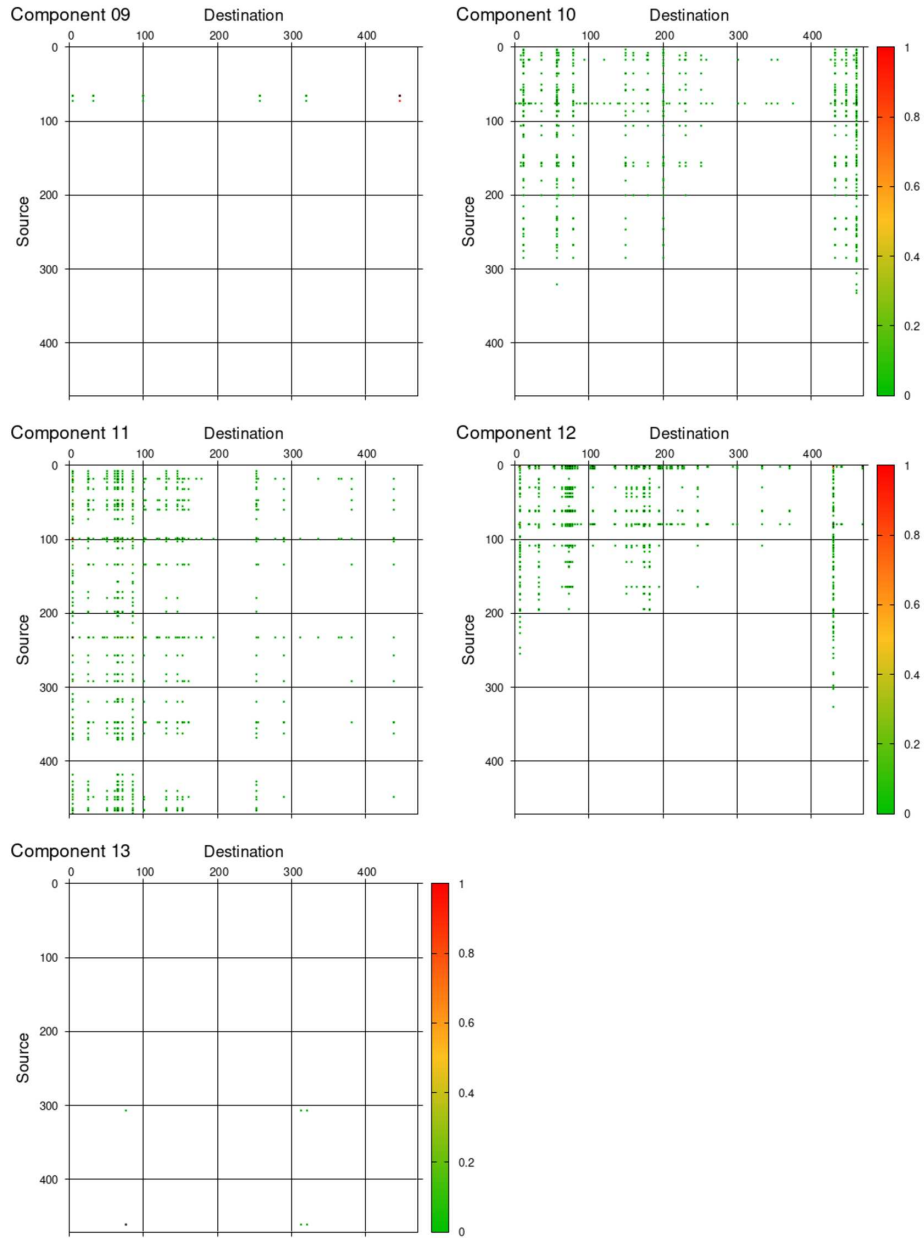
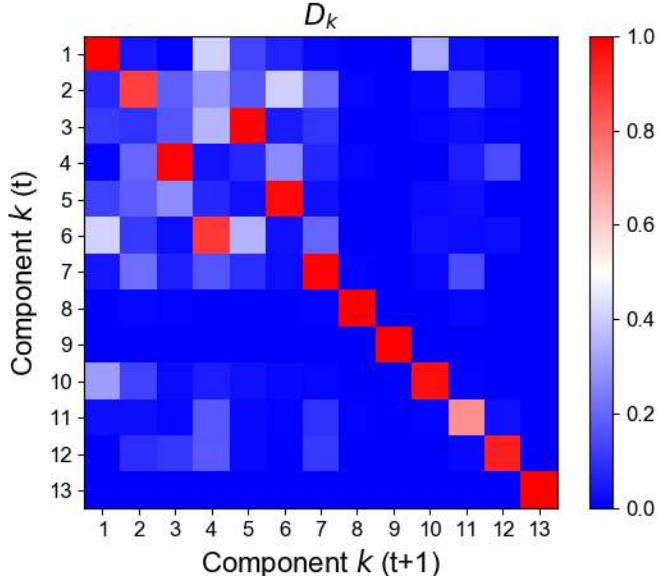
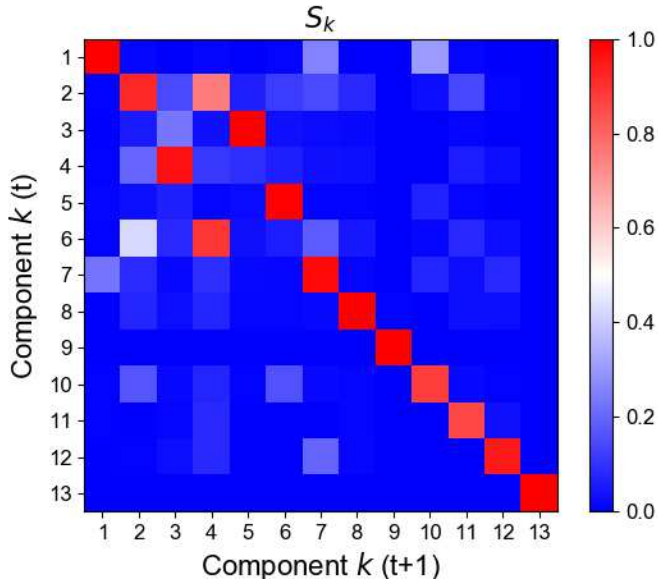


**Fig. 13.** (Continued) NMF components  $k = 9, \dots, 13$  as matrices defined by  $\widetilde{S}_{sk} \widetilde{D}_{kd}$  in (32). Data: 2019-09.



(a) Cosine similarity of NMF basis vectors  $D_k$



(b) Cosine similarity of NMF basis vectors  $S_k$

**Fig. 14.** Temporal change of the NMF components from one month  $t$  to its successive month  $t + 1$ . (a) Cosine similarities calculated for all the pairs of  $D_k$  ( $k = 1, \dots, 13$ ) between  $t$  (vertical) and  $t + 1$ . (b) The same for all the pairs of  $S_k$ . For the vertical and horizontal axes in (a) and (b), the order of indices along vertical and horizontal axes corresponds to the descending order of the probability  $r_k$  in (31). Data: 2019-09 and 2019-10.

## 4. Discussions

Let us briefly discuss about several aspects that would be worth further investigation.

First, while we succeeded to extract the NMF components and found that the components have non-zero values only at a relatively small number of users, we still did not identify those users by exploiting the fact. It is quite likely the case that the extracted users must play important roles in each of the NMF components, either of key destinations or key sources. We attempted to identify a tiny fraction of such users by matching the list of such users with the identity given in Appendix A, but the identification was not sufficient in order to interpret the meaning of corresponding NMF components. Instead, such intra-day activities as shown in Fig. 2 of Section 2.1 could give us the geographical locations of those key users, possibly uncovering the crypto flow in each NMF component at a global scale. This issue remains to be investigated.

Second, even if the temporal change of the network in terms of the NMF components has such a stable structure as found in Fig. 14, we noticed that there exists interesting change of a few components in the same figure. A keen reader may have noticed that the components  $k = 3, 4, 5, 6$  at time  $t$  are changed into among themselves at time  $t + 1$ , while the cosine similarities are close to 1. This means that the probabilities  $r_k$  for those components were changed from one month to the next. Also one can notice that the optimal number of NMF components showed a slow variation during the period (recall Table D-1 of Appendix D). These facts might give us a hint for how to treat the temporal change of network by paying attention to those slowly varying aspects. Additionally, while we focused only on regular users appearing everyday during the period under study, it would be necessary to include the process of entry and exit of big players.

Third, technically, we regarded the method of NMF as a probabilistic model that shares the same stochastic process as in the probabilistic latent semantic analysis (PLSA). As a bonus, we were able to employ the latent Dirichlet allocation (LDA) and its known methods to estimate the number of topics in the context of topic model, or the number of NMF components in our context. In principle, one could start with the full-fledged Bayesian framework in the LDA and its extension and variations. It would be worth pursuing in this direction, which is also related to the second point above, because there are several studies on how to treat temporally changing topics of documents in a long time-span.

Fourth, our methods in this paper can be easily applied to different cryptoassets including Ethereum and XRP. We are aware of the paper [20] in this volume, which is in a similar line of study. It would be interesting to apply our methods to the data of XRP.

Finally, it would be an extremely interesting problem how the crypto flow among big players is related to the *prices* in the exchange markets with fiat currencies and also with other cryptoassets. It is quite likely that the bubble/crash and their precursors might force the big players to react during such turmoils in a different way from tranquil periods. For example, exchanges need to reallocate cryptoassets in the necessity of making a reservoir or doing a release of cryptoassets under the risk.

## 5. Summary

Our purpose in this study on the cryptoasset of Bitcoin is to understand the structure and temporal change of crypto flow among big players. We compiled all the transactions contained in the blockchain of Bitcoin cryptoasset from its genesis to the year 2020, identified users from anonymous addresses, and constructed snapshots of networks comprising of users as nodes and links as crypto flow among the users. While the whole network is huge, we extracted sub-networks by focusing on regular users who appeared persistently during a certain period. Specifically, we extracted monthly snapshots during the year of 2019, and selected roughly 500 regular users.

We first analyzed the bow-tie structure from the binary relationship of flow, and then performed the Hodge decomposition based on the strength of flow defined by frequencies and amounts, in order

to locate users in the upstream, downstream, and core of the entire crypto flow. We found that the bow-tie structure is stable during the period, implying that those regular users have different roles in the crypto flow.

Then, to reveal important ingredients hidden in the flow, we employ the method of non-negative matrix factorization (NMF) to extract a set of principal components. We discussed that the NMF method can be regarded as a probabilistic model, which is equivalent to a probabilistic latent semantic analysis and its typical model of latent Dirichlet allocation. This observation brought us a method to estimate an optimal number of NMF components, which turned out to be a dozen or so. We found that the NMF components have non-zero values corresponding to a limited number of users, telling us their roles of destinations or sources of the crypto flow. Additionally, we found that the NMF components are quite stable in the temporal change for the time-scale of months.

There remain several points including the further investigation on the users contained in those NMF components, a treatment of temporally changing network, and technically interesting issues to be pursued in the future.

## Acknowledgment

We would like to thank Hideaki Aoyama, Yuichi Ikeda, and Hiwon Yoon for discussions, Hiroshi Iyetomi for solving a technical issue of Hodge decomposition, Itsuki Noda for clarifying his application of NMF on transportation data, Takeaki Uno for an efficient algorithm to identify users, Shinya Kawata and Wajun Kawai for technical assistance. This work is supported by JSPS KAKENHI Grant Numbers, 19K22032 and 20H02391, by the Nomura Foundation (Grants for Social Science), and also by Kyoto University and Ripple’s collaboration scheme.

## References

- [1] F. Reid and M. Harrigan. An analysis of anonymity in the bitcoin system. In Y. Altshuler, Y. Elovici, A. Cremers, N. Aharony, and A. Pentland, editors, *Security and Privacy in Social Networks*, pages 197–223. Springer, New York, 2013.
- [2] M. Ober, S. Katzenbeisser, and K. Hamacher. Structure and anonymity of the bitcoin transaction graph. *Future Internet*, **5**(2):237–250, 2013.
- [3] D. Ron and A. Shamir. Quantitative analysis of the full bitcoin transaction graph. In *Financial Cryptography and Data Security*, 2013.
- [4] D. Kondor, M. Pósfai, I. Csabai, and G. Vattay. Do the rich get richer? an empirical analysis of the bitcoin transaction network. *PLoS ONE*, **9**(2):e86197, 2014.
- [5] D. Kondor, I. Csabai, S. J., M. Pósfai, and G. Vattay. Inferring the interplay between network structure and market effects in bitcoin. *New Journal of Physics*, **16**(12):125003, 2014.
- [6] B. Alvarez-Pereira, M. A. Ayres, A. M. G. López, S. Gorsky, S. W. Hayes, Z. Qiao, and J. Santana. Network and conversation analyses of bitcoin. In *2014 Complex Systems Summer School Proceedings*, 2014.
- [7] A. Baumann, B. Fabian, and M. Lischke. Exploring the bitcoin network. In *Proceedings of the 10th International Conference on Web Information Systems and Technologies – Volume 2: WEBIST*, 2014.
- [8] M. Fleder, M. S. Kester, and S. Pillai. Bitcoin transaction graph analysis. <http://arxiv.org/abs/1502.01657>, 2015.
- [9] D. Maesa, A. Marino, and L. Ricci. Uncovering the bitcoin blockchain: An analysis of the full users graph. In *Conference: 2016 IEEE International Conference on Data Science and Advanced Analytics (DSAA)*, 2016.
- [10] M. Lischke and B. Fabian. Analyzing the bitcoin network: The first four years. *Future Internet*, **8**(1):7, 2016.
- [11] C. G. Akcora, Y. R. Gel, and M. Kantarcioglu. Blockchain: A graph primer. <http://arxiv.org/abs/1708.08749>, 2017.
- [12] M. Bartoletti, A. Bracciali, S. Lande, and L. Pompianu. A general framework for bitcoin analytics. <http://arxiv.org/abs/1707.01021>, 2017.

- [13] C. Cachin, A. D. Caro, P. Moreno-Sanchez, B. Tackmann, and M. Vukolić. The transaction graph for modeling blockchain semantics. <https://eprint.iacr.org/2017/1070>, 2017.
- [14] R. Cazabet, B. Rym, and M. Latapy. Tracking bitcoin users activity using community detection on a network of weak signals. <http://arxiv.org/abs/1710.08158>, 2017.
- [15] D. Maesa, A. Marino, and L. Ricci. Data-driven analysis of bitcoin properties: exploiting the users graph. *International Journal of Data Science and Analytics*, 2017.
- [16] S. Ranshous, C. Joslyn, S. Kreyling, K. Nowak, N. F. Samatova, C. L. West, and S. Winters. Exchange pattern mining in the bitcoin transaction directed hypergraph. In *Financial Cryptography Workshops*, 2017.
- [17] A. M. Antonopoulos. *Mastering Bitcoin: Programming the Open Blockchain*. O’Reilly Media, 2 edition, 2017.
- [18] Hungary research group: Elte bitcoin project. <http://www.vo.elte.hu/bitcoin/>; <https://senseable2015-6.mit.edu/bitcoin/>. Accessed: 2020-01-03.
- [19] Bitcoin block explorer with address grouping and wallet labeling. <https://www.walletexplorer.com>. Accessed: 2021-03-18.
- [20] H. Aoyama. Xrp network and proposal of flow index; see it in this volume., 2021.
- [21] R. Islam, Y. Fujiwara, S. Kawata, and H. Yoon. Analyzing outliers activity from the time-series transaction pattern of bitcoin blockchain. *Evolutionary and Institutional Economics Review*, **16**(1):239–257, 2019.
- [22] R. Islam, Y. Fujiwara, S. Kawata, and H. Yoon. Unfolding identity of financial institutions in bitcoin blockchain by weekly pattern of network flows. in preparation, 2020.
- [23] A. Broder, R. Kumar, F. Maghoul, P. Raghavan, S. Rajagopalan, R. Stata, A. Tomkins, and J. Wiener. Graph structure in the Web. *Computer Networks*, **33**(1-6):309–320, 2000.
- [24] X. Jiang, L.-H. Lim, Y. Yao, and Y. Ye. Learning to rank with combinatorial hodge theory. available online, 2008. accessed in January, 2020.
- [25] X. Jiang, L.-H. Lim, Y. Yao, and Y. Ye. Statistical ranking and combinatorial hodge theory. *Mathematical Programming*, **127**(1):203–244, 2011.
- [26] J. L. Johnson. Discrete hodge theory on graphs: a tutorial. *Computing in Science & Engineering*, **15**(5):42–55, 2013.
- [27] K. Miura and T. Aoki. Scaling of hodge-kodaira decomposition distinguishes learning rules of neural networks. *IFAC-PapersOnLine*, **48**(18):175–180, 2015.
- [28] Y. Kichikawa, H. Iyetomi, T. Iino, and H. Inoue. Hierarchical and circular flow structure of interfirm transaction networks in japan. <https://ssrn.com/abstract=3173955>, 2018. May 4, 2018.
- [29] Y. Fujiwara, H. Inoue, T. Yamaguchi, H. Aoyama, T. Tanaka, and K. Kikuchi. Money flow network among firms’ accounts in a regional bank of japan. *EPJ Data Science*, **10**:19, 2021.
- [30] F. Y. and I. R. *Advanced Studies of Financial Technologies and Cryptocurrency Markets*, chapter Hodge Decomposition of Bitcoin Money Flow. Springer, Singapore, 2020.
- [31] D. D. Lee and H. S. Seung. Learning the parts of objects by non-negative matrix factorization. *Nature*, **401**(6755):788–791, 1999.
- [32] M. W. Berry, M. Browne, A. N. Langville, V. P. Pauca, and R. J. Plemmons. Algorithms and applications for approximate nonnegative matrix factorization. *Computational Statistics & Data Analysis*, **52**(1):155–173, 2007.
- [33] R. Gaujoux and C. Seoighe. A flexible r package for nonnegative matrix factorization. *BMC Bioinformatics*, **11**:367, 2010.
- [34] H. Kameoka. Non-negative matrix factorization and its variants with applications to audio signal processing. *Journal of the Japan Statistical Society*, **44**(2):383–407, 2015. Japanese.
- [35] I. Noda and J. Ochiai. Analysis of od data of ondemand transportation by non-negative matrix factorization. 2019. Technical report in the workshop of SIG-DOCMAS, Japanese.
- [36] T. Hofmann. Unsupervised learning by probabilistic latent semantic analysis. *Machine Learning*, **42**:177–196, 2001.
- [37] T. L. Griffiths and M. Steyvers. Finding scientific topics. *Proceedings of the National Academy of Sciences*, **101**:5228–5235, 2004.
- [38] J. Cao, T. Xia, J. Li, Y. Zhang, and S. Tang. A density-based method for adaptive lda model selection. *Neurocomputing*, **72**(7):1775–1781, 2009.



- [39] R. Arun, V. Suresh, C. E. Veni Madhavan, and M. N. Narasimha Murthy. On finding the natural number of topics with latent dirichlet allocation: Some observations. In M. J. Zaki, J. X. Yu, B. Ravindran, and V. Pudi, editors, *Advances in Knowledge Discovery and Data Mining*, pages 391–402. Springer Berlin Heidelberg, 2010.
- [40] R. Deveaud, E. SanJuan, and P. Bellot. Accurate and effective latent concept modeling for ad hoc information retrieval. *Document Numérique*, **17**(1):61–84, 2014.
- [41] D. M. Blei, A. Y. Ng, and M. I. Jordan. Latent dirichlet allocation. *Journal of Machine Learning Research*, **3**:993–1022, 2003.
- [42] D. M. Blei and J. D. Lafferty. *Text Mining: Classification, Clustering, and Applications*, chapter Topic Models, pages 71–94. CRC Press, 2009.
- [43] Grün, Bettina and Hornik, Kurt. **topicmodels**: An R Package for Fitting Topic Models. *Journal of Statistical Software*, **40**(13):1–30, 2011.
- [44] Y. W. Teh, M. I. Jordan, M. J. Beal, and D. M. Blei. Hierarchical dirichlet processes. *Journal of the American Statistical Association*, **101**(476):1–30, 2006.

## Appendix A: Identity of Users of Type A

WalletExplorer.com [19] is a web site providing information about identity of addresses in Bitcoin blockchain. The site merges addresses together, if they are part of the same wallet, and also identifies wallets with actual names. According to the site, the method to merge addresses is:

*Just a basic algorithm is used to determine wallet addresses. Addresses are merged together, if they are co-spent in one transaction. So if addresses A and B are co-spent in transaction T1, and addresses B and C are co-spent in transaction T2, all addresses A, B and C will be part of one wallet.*

*Sometimes, an address belongs to some service but it was never co-spent with others. Then that address stays unnamed. It is typically more often at addresses with higher amount (as there is no need to co-spending).*

This method is precisely the same as [1], which is the one we employed in Section 2.1. In addition, the identification of actual names is done by WalletExplorer.com as follows:

*In most of the cases, I registered to service, made transaction(s) and saw which wallet bitcoins were merged with, or from which wallet it was withdrawn.*

*There is probably no easier way how to discover names other than this.*

*Please note that the name database is not updated, so it does not contain newer exchanges (or newer wallets of existing exchanges).*

We matched our data with the one in [19] to obtain the identity and additional attributes of users of type A (see Section 2.1 for the type). Table A-1 is the classification into exchanges, services, gambling, historic, and mining pools. Table A-2 shows the list of countries that exchanges belong to. Table A-3 is the complete list of this matching.

**Table A-1.** Classification of identified users (compiled from [19])

Classification	#Users	Examples
Exchanges	84	Bittrex.com, Huobi.com, Bit-x.com, HitBtc.com
Old/Historic	83	AgoraMarket, EvolutionMarket, SilkRoadMarketplace
Services/Others	45	Xapo.com, ePay.info, Cubits.com
Gambling	41	999Dice.com, CoinGaming.io, SatoshiMines.com
Pools	11	BTCCPool, SlushPool.com, BitMinter.com
Total	264	—

**Table A-2.** Countries of identified exchanges (compiled from [19])

Country	#Users	Country	#Users	Country	#Users
China	14	Mexico	2	Iran	1
UK	13	Netherlands	2	Korea	1
USA	13	Poland	2	Luxembourg	1
Canada	4	Portugal	2	Malta	1
Australia	3	South Africa	2	Panama	1
Brazil	3	Austria	1	Taiwan	1
Singapore	3	Belize	1	Thailand	1
Russia	3	Croatia	1	Vanuatu	1
Denmark	2	Czech	1	Vietnam	1
Finland	2	Germany	1	Total	84

**Table A.3.:** Identity of Users (compiled from [19])

Definitions

No: sequential number

User ID: an arbitrarily but uniquely assigned IDs to each user in our data

#Addr. (1): number of addresses identified to each User ID in our data (rows are sorted by this column)

#Addr. (2): the same as (1) but provided by WalletExplorer.com (at the timing of writing)

No.	User ID	#Addr. (1)	#Addr. (2)	Name	Category	Country
1	0000000000	18,913,420	1	Bit-x.com	Exchanges	South Africa
2	0000000000	18,913,420	1	Xapo.com	Services/Others	—
3	0000000001	13,110,033	12,469,250	ePay.info	Services/Others	—
4	0000000002	5,302,867	1	Cryptopay.me	Services/Others	—
5	0000000002	5,302,867	1	Cubits.com	Services/Others	—
6	0000000002	5,302,867	1	Luno.com	Exchanges	South Africa
7	0000000002	5,302,867	1	VirWoX.com	Exchanges	Austria
8	0000000002	5,302,867	1	Xapo.com	Services/Others	—
9	0000000002	5,302,867	487,776	CoinPayments.net	Services/Others	—
10	0000000006	2,180,236	1,488,034	Xapo.com	Services/Others	—
11	0000000010	1,630,483	1	Huobi.com	Exchanges	China
12	0000000010	1,630,483	957,652	Cubits.com	Services/Others	—
13	0000000011	1,538,476	1,377,461	Bittrex.com	Exchanges	USA
14	0000000012	1,413,904	1	Bitstamp.net	Exchanges	Luxembourg
15	0000000014	1,043,379	279,697	Huobi.com	Exchanges	China
16	0000000017	992,726	1	VirWoX.com	Exchanges	Austria
17	0000000017	992,726	1	Xapo.com	Services/Others	—
18	0000000018	988,300	940,605	Poloniex.com	Exchanges	USA
19	0000000022	912,950	133,020	AnxPro.com	Exchanges	China
20	0000000022	912,950	770,486	CoinTrader.net	Exchanges	Canada
21	0000000025	845,559	1	Cubits.com	Services/Others	—
22	0000000028	811,809	2	Cubits.com	Services/Others	—
23	0000000030	778,990	651,547	999Dice.com	Gambling	—
24	0000000035	682,176	1	MoonBit.co.in	Services/Others	—
25	0000000037	659,820	656,699	CoinGaming.io	Gambling	—
26	0000000038	631,985	1	Luno.com	Exchanges	South Africa
27	0000000041	581,525	1	Cubits.com	Services/Others	—
28	0000000042	546,515	291,443	Luno.com	Exchanges	South Africa
29	0000000043	523,330	522,056	LocalBitcoins.com	Exchanges	Finland
30	0000000045	498,001	498,001	AgoraMarket	Old/Historic	—
31	0000000049	478,476	343,039	Bitstamp.net	Exchanges	Luxembourg
32	0000000054	420,632	420,632	EvolutionMarket	Old/Historic	—
33	0000000055	412,338	249,883	Cryptonator.com	Services/Others	—
34	0000000057	398,349	1	Xapo.com	Services/Others	—
35	0000000060	377,140	305,518	Cryptopay.me	Services/Others	—
36	0000000061	372,753	372,753	SilkRoadMarketplace	Old/Historic	—
37	0000000063	350,036	350,036	SilkRoad2Market	Old/Historic	—
38	0000000069	341,160	61,103	MercadoBitcoin.com.br	Exchanges	Brazil
39	0000000071	325,365	1	Xapo.com	Services/Others	—
40	0000000075	307,489	307,451	BTC-e.com	Exchanges	Russia
41	0000000077	294,238	1	Xapo.com	Services/Others	—
42	0000000079	278,973	2	Cubits.com	Services/Others	—
43	0000000082	266,695	254,601	SatoshiMines.com	Gambling	—
44	0000000083	263,074	262,940	YoBit.net	Exchanges	Russia
45	0000000086	250,920	191,689	Bitcoin.de	Exchanges	Germany
46	0000000090	241,250	223,781	BitcoinFog	Services/Others	—
47	0000000093	238,480	238,476	Cex.io	Exchanges	UK
48	0000000101	206,542	156,203	CoinJar.com	Services/Others	—
49	0000000107	197,164	197,155	NitrogenSports.eu	Gambling	—
50	0000000114	189,776	189,776	AlphaBayMarket	Services/Others	—
51	0000000116	187,189	187,086	HitBtc.com	Exchanges	UK
52	0000000120	186,000	186,000	BitPay.com	Services/Others	—
53	0000000135	168,885	1	Luno.com	Exchanges	South Africa
54	0000000158	146,381	146,381	NucleusMarket	Services/Others	—
55	0000000159	145,978	1	Cryptonator.com	Services/Others	—
56	0000000159	145,978	1	Cubits.com	Services/Others	—
57	0000000169	140,594	1	Bitcoin.de	Exchanges	Germany

*Continue to next page*

Table A-3 continued from previous page

No.	User ID	#Addr. (1)	#Addr. (2)	Name	Category	Country
58	0000000169	140,594	1	Cubits.com	Services/Others	—
59	0000000169	140,594	1	Poloniex.com	Exchanges	USA
60	0000000176	134,559	134,559	Cryptsy.com	Exchanges	USA
61	0000000182	131,979	1	Poloniex.com	Exchanges	USA
62	0000000190	125,004	125,004	PocketDice.io	Gambling	—
63	0000000195	122,249	1	Bitstamp.net	Exchanges	Luxembourg
64	0000000199	120,548	120,491	FortuneJack.com	Gambling	—
65	0000000201	119,119	119,065	AbraxasMarket	Old/Historic	—
66	0000000208	115,775	115,775	CoinKite.com	Services/Others	—
67	0000000210	114,458	114,458	Kraken.com	Exchanges	USA
68	0000000216	109,798	1	Luno.com	Exchanges	South Africa
69	0000000217	109,151	109,151	Instawallet.org	Old/Historic	—
70	0000000219	107,479	85,122	Bleutrade.com	Exchanges	Brazil
71	0000000234	96,890	96,890	SecondsTrade.com	Gambling	—
72	0000000239	92,226	72,581	HolyTransaction.com	Services/Others	—
73	0000000244	90,473	44,416	CoinSpot.com.au	Exchanges	Australia
74	0000000252	85,637	85,626	MintPal.com	Old/Historic	—
75	0000000253	85,566	84,679	Hashnest.com	Exchanges	China
76	0000000259	83,723	83,517	BtcTrade.com	Exchanges	China
77	0000000263	82,695	27,343	BTCJam.com	Services/Others	—
78	0000000267	80,987	73,965	OKCoin.com	Exchanges	China
79	0000000269	80,086	1	Poloniex.com	Exchanges	USA
80	0000000270	79,712	79,712	Bter.com	Exchanges	China
81	0000000274	78,849	78,849	BitZino.com	Gambling	—
82	0000000278	78,119	78,048	OKCoin.com	Exchanges	China
83	0000000282	76,997	1	Cubits.com	Services/Others	—
84	0000000282	76,997	52,925	BitoEX.com	Services/Others	—
85	0000000286	74,602	74,602	Rollin.io	Gambling	—
86	0000000300	68,956	67,795	CloudBet.com	Gambling	—
87	0000000302	68,658	55,098	VirWoX.com	Exchanges	Austria
88	0000000307	67,114	1	Cubits.com	Services/Others	—
89	0000000312	66,748	1	Luno.com	Exchanges	South Africa
90	0000000318	65,367	1	VirWoX.com	Exchanges	Austria
91	0000000325	64,803	64,803	BTCC.com	Exchanges	China
92	0000000347	57,770	57,753	MaiCoin.com	Exchanges	Taiwan
93	0000000350	56,952	56,952	BTCCPool	Pools	—
94	0000000358	55,757	55,757	PandoraOpenMarket	Old/Historic	—
95	0000000359	55,703	1	MercadoBitcoin.com.br	Exchanges	Brazil
96	0000000362	55,167	55,167	Paxful.com	Exchanges	USA
97	0000000366	54,640	54,640	PrimeDice.com	Gambling	—
98	0000000370	53,639	53,639	SheepMarketplace	Old/Historic	—
99	0000000374	53,102	53,102	Cavirtex.com	Exchanges	Canada
100	0000000387	50,878	50,878	BlackBankMarket	Old/Historic	—
101	0000000402	48,602	48,518	BX.in.th	Exchanges	Thailand
102	0000000403	48,525	19,434	MoonBit.co.in	Services/Others	—
103	0000000407	48,178	33,372	HaoBTC.com	Services/Others	—
104	0000000412	47,295	47,281	Matbea.com	Exchanges	UK
105	0000000444	42,750	41,150	SatoshiDice.com	Gambling	—
106	0000000447	42,327	41,866	BitcoinWallet.com	Services/Others	—
107	0000000468	40,270	1	Cubits.com	Services/Others	—
108	0000000480	39,013	1	VirWoX.com	Exchanges	Austria
109	0000000482	38,880	1	Huobi.com	Exchanges	China
110	0000000501	36,999	36,999	Justcoin.com	Old/Historic	—
111	0000000508	35,537	1	Bitcoin.de	Exchanges	Germany
112	0000000508	35,537	28,567	SafeDice.com	Gambling	—
113	0000000511	35,453	35,453	McxNOW.com	Old/Historic	—
114	0000000512	35,433	35,433	C-Cex.com	Exchanges	UK
115	0000000527	34,149	34,149	MiddleEarthMarketplace	Old/Historic	—
116	0000000533	33,436	33,389	VirCurex.com	Exchanges	China
117	0000000537	32,823	32,823	Purse.io	Services/Others	—
118	0000000539	32,701	32,701	SatoshiBet.com	Gambling	—
119	0000000542	32,017	27,693	SwCPoker.eu	Gambling	—
120	0000000545	31,940	30,755	BitBargain.co.uk	Exchanges	UK
121	0000000556	30,965	30,965	SealsWithClubs.eu	Old/Historic	—

Continue to next page

Table A-3 continued from previous page

No.	User ID	#Addr. (1)	#Addr. (2)	Name	Category	Country
122	0000000559	30,624	22,599	BlockTrades.us	Exchanges	USA
123	0000000562	30,251	16,052	CoinMotion.com	Exchanges	Finland
124	0000000563	30,187	30,183	OkLink.com	Services/Others	—
125	0000000571	29,256	29,256	Huobi.com	Exchanges	China
126	0000000591	27,653	23,515	Bit-x.com	Exchanges	South Africa
127	0000000605	26,622	26,622	BtcDice.com	Old/Historic	—
128	0000000614	26,013	24,204	BitBay.net	Exchanges	Poland
129	0000000615	25,960	25,960	Betcoin.ag	Gambling	—
130	0000000626	25,257	1	Cubits.com	Services/Others	—
131	0000000649	23,841	20,866	Paymium.com	Services/Others	—
132	0000000672	22,597	22,597	Loanbase.com	Services/Others	—
133	0000000676	22,304	22,304	Coinroll.com	Gambling	—
134	0000000687	21,693	21,693	FaucetBOX.com	Services/Others	—
135	0000000690	21,640	10,439	CoinHako.com	Exchanges	Singapore
136	0000000717	20,484	18,001	FYBSG.com	Exchanges	Singapore
137	0000000747	19,810	19,605	TheRockTrading.com	Exchanges	Malta
138	0000000762	18,997	18,997	BlueSkyMarketplace	Old/Historic	—
139	0000000774	18,489	18,489	Crypto-Games.net	Gambling	—
140	0000000794	17,705	17,705	Coin-Swap.net	Old/Historic	—
141	0000000804	17,531	1	Luno.com	Exchanges	South Africa
142	0000000869	15,965	15,965	AnoniBet.com	Gambling	—
143	0000000874	15,905	15,905	ChangeTip.com	Services/Others	—
144	0000000881	15,757	15,757	Bitmit.net	Old/Historic	—
145	0000000891	15,495	15,495	CoinApult.com	Services/Others	—
146	0000000902	15,260	15,260	BtcMarkets.net	Exchanges	Australia
147	0000000926	14,566	14,566	Inputs.io	Old/Historic	—
148	0000000934	14,394	1	Huobi.com	Exchanges	China
149	0000000959	13,713	11,210	Vaultoro.com	Exchanges	UK
150	0000001006	12,486	12,486	CryptoStocks.com	Services/Others	—
151	0000001007	12,456	12,456	BitAces.me	Old/Historic	—
152	0000001071	11,221	11,221	Coins-e.com	Exchanges	Canada
153	0000001072	11,220	11,220	Igot.com	Exchanges	Belize
154	0000001093	10,901	10,900	SatoshiRoulette.com	Gambling	—
155	0000001177	9,667	1	Bittrex.com	Exchanges	USA
156	0000001199	9,512	9,512	Crypto-Trade.com	Old/Historic	—
157	0000001235	9,165	9,165	Cryptorush.in	Old/Historic	—
158	0000001240	9,122	9,122	BTCOracle.com	Gambling	—
159	0000001255	8,967	8,967	Genesis-Mining.com	Services/Others	—
160	0000001313	8,430	8,430	Exmo.com	Exchanges	UK
161	0000001325	8,371	4,343	SlushPool.com	Pools	—
162	0000001355	8,120	8,120	Vault0fSatoshi.com	Old/Historic	—
163	0000001368	8,032	8,032	BitcoinVideoCasino.com	Gambling	—
164	0000001393	7,865	7,865	BTCGuild.com	Old/Historic	—
165	0000001395	7,857	7,766	Peerbet.org	Gambling	—
166	0000001397	7,848	7,848	796.com	Exchanges	Vanuatu
167	0000001421	7,585	7,585	Btc38.com	Exchanges	UK
168	0000001438	7,479	7,479	Betcoins.net	Old/Historic	—
169	0000001497	7,109	7,109	LiteBit.eu	Exchanges	Netherlands
170	0000001568	6,788	6,207	Bitbond.com	Services/Others	—
171	0000001588	6,669	5,369	HappyCoins.com	Exchanges	Netherlands
172	0000001631	6,477	6,477	Bitcoin-Roulette.com	Old/Historic	—
173	0000001666	6,309	6,309	AllCoin.com	Old/Historic	—
174	0000001685	6,242	6,242	Coin.mx	Old/Historic	—
175	0000001739	6,009	4,726	LakeBTC.com	Exchanges	China
176	0000001750	5,966	5,966	777Coin.com	Gambling	—
177	0000001760	5,934	5,934	GHash.io	Pools	—
178	0000001796	5,762	5,762	DoctorDMarket	Services/Others	—
179	0000001862	5,481	5,481	Coinomat.com	Exchanges	UK
180	0000001916	5,297	5,295	Coinmate.io	Exchanges	UK
181	0000002012	5,024	5,024	BitVC.com	Exchanges	China
182	0000002024	4,996	4,875	SatoshiCircle.com	Gambling	—
183	0000002039	4,953	1	Luno.com	Exchanges	South Africa
184	0000002055	4,896	4,896	MyBitcoin.com	Old/Historic	—
185	0000002098	4,775	4,775	AllCrypt.com	Old/Historic	—

Continue to next page

Table A-3 continued from previous page

No.	User ID	#Addr. (1)	#Addr. (2)	Name	Category	Country
186	0000002155	4,629	4,629	GermanPlazaMarket	Services/Others	—
187	0000002169	4,605	4,605	MasterXchange.com	Old/Historic	—
188	0000002183	4,551	4,272	CoinCafe.com	Exchanges	USA
189	0000002192	4,530	4,242	BitKonan.com	Exchanges	Croatia
190	0000002197	4,516	4,516	QuadrigaCX.com	Exchanges	Canada
191	0000002216	4,451	4,451	BitElfin.com	Old/Historic	—
192	0000002243	4,377	4,377	OrderBook.net	Exchanges	USA
193	0000002251	4,363	3,800	SpectroCoin.com	Exchanges	UK
194	0000002259	4,354	4,354	Bitcurex.com	Exchanges	Poland
195	0000002265	4,338	4,338	Coinchiwa.com	Gambling	—
196	0000002281	4,292	4,277	Betcoin.tm	Gambling	—
197	0000002305	4,232	4,227	MeXBT.com	Exchanges	Mexico
198	0000002403	3,999	3,999	Bitfinex.com	Exchanges	China
199	0000002424	3,947	1,571	CoinVault	Old/Historic	—
200	0000002464	3,861	3,861	BetsOfBitco.in	Old/Historic	—
201	0000002471	3,840	3,840	JetWin.com	Gambling	—
202	0000002587	3,607	3,607	BitZillions.com	Gambling	—
203	0000002617	3,545	3,543	Korbit.co.kr	Exchanges	Korea
204	0000002661	3,485	3,485	BTCPop.co	Services/Others	—
205	0000002849	3,216	2,181	YABTCL.com	Gambling	—
206	0000002922	3,121	3,121	BIToomBa.com	Old/Historic	—
207	0000002952	3,086	3,086	BitYes.com	Old/Historic	—
208	0000002965	3,075	2,640	BetMoose.com	Gambling	—
209	0000003031	2,979	2,978	CoinURL.com	Services/Others	—
210	0000003139	2,829	2,829	CannabisRoadMarket	Old/Historic	—
211	0000003195	2,760	2,760	Ice-Dice.com	Old/Historic	—
212	0000003211	2,744	2,744	ChBtc.com	Exchanges	China
213	0000003249	2,713	2,713	CoinArch.com	Exchanges	Singapore
214	0000003310	2,645	2,645	Comkort.com	Old/Historic	—
215	0000003340	2,618	2,618	BitNZ.com	Services/Others	—
216	0000003348	2,614	2,614	CleverCoin.com	Exchanges	USA
217	0000003388	2,575	2,575	CoinMkt.com	Old/Historic	—
218	0000003637	2,355	2,355	DiceBitco.in	Old/Historic	—
219	0000003756	2,276	2,276	BitcoinVietnam.com.vn	Exchanges	Vietnam
220	0000003840	2,221	2,221	Indacoin.com	Exchanges	UK
221	0000004134	2,023	2,023	BitClix.com	Services/Others	—
222	0000004187	1,992	1,992	Coin-Sweeper.com	Old/Historic	—
223	0000004271	1,948	1,948	GoCelery.com	Services/Others	—
224	0000004570	1,812	1,812	Playt.in	Old/Historic	—
225	0000004580	1,804	1,796	Bitcash.cz	Old/Historic	—
226	0000004586	1,802	1,802	CampBX.com	Exchanges	USA
227	0000004817	1,713	1,713	BTCLend.org	Services/Others	—
228	0000004840	1,704	1,704	CoinChimp.com	Exchanges	Russia
229	0000004863	1,699	1,699	BtcExchange.ro	Old/Historic	—
230	0000004882	1,690	1,690	AdmiralCoin.com	Old/Historic	—
231	0000005002	1,643	1,643	Bitcoinica.com	Old/Historic	—
232	0000005121	1,594	1,594	Gatecoin.com	Exchanges	China
233	0000005399	1,508	1,508	BetChain.com-old	Gambling	—
234	0000005547	1,471	1,471	BabylonMarket	Old/Historic	—
235	0000005637	1,443	1,443	HelixMixer	Services/Others	—
236	0000006104	1,314	1,314	Bylls.com	Services/Others	—
237	0000006381	1,246	1,246	Btcst.com-pirateat40	Old/Historic	—
238	0000006688	1,189	1,189	PocketRocketsCasino.eu	Old/Historic	—
239	0000006697	1,188	1,188	Bitso.com	Exchanges	Mexico
240	0000006747	1,178	1,178	BTct.com	Old/Historic	—
241	0000006753	1,176	1,176	DaDice.com	Old/Historic	—
242	0000007201	1,095	1,095	Cryptonit.net	Exchanges	UK
243	0000007312	1,076	1,076	BitStarz.com	Gambling	—
244	0000007547	1,040	1,040	Ccedk.com	Exchanges	Denmark
245	0000007673	1,020	1,020	Satoshi-Karoshi.com	Gambling	—
246	0000007783	1,005	1	VirWoX.com	Exchanges	Austria
247	0000008133	978	978	Just-Dice.com	Old/Historic	—
248	0000008213	968	968	CryptoLocker	Old/Historic	—
249	0000008232	965	965	GreenRoadMarket	Services/Others	—

Continue to next page

Table A-3 continued from previous page

No.	User ID	#Addr. (1)	#Addr. (2)	Name	Category	Country
250	0000008325	953	953	CoinRoyale.com	Gambling	—
251	0000008352	950	950	CryptoBounty.com	Old/Historic	—
252	0000009025	876	876	1Coin.com	Exchanges	China
253	0000009100	869	679	Coingi.com	Exchanges	Panama
254	0000010744	746	746	BitcoinWeBank.com	Old/Historic	—
255	0000010833	741	741	EmpoEX.com	Exchanges	USA
256	0000011035	729	729	FairProof.com	Gambling	—
257	0000011546	700	700	UseCryptos.com	Exchanges	Portugal
258	0000011749	686	1	Cubits.com	Services/Others	—
259	0000011857	681	1	VirWoX.com	Exchanges	Austria
260	0000012513	670	669	AntPool.com	Pools	—
261	0000012569	668	668	Coinbroker.io	Exchanges	USA
262	0000012639	665	665	UpDown.BT	Old/Historic	—
263	0000013022	648	648	DiceNow.com	Gambling	—
264	0000013139	643	643	Dagensia.eu	Old/Historic	—
265	0000013870	614	614	WatchMyBit.com	Services/Others	—
266	0000014175	604	604	MPEX.co	Old/Historic	—
267	0000014703	593	593	Banx.io	Exchanges	USA
268	0000015353	572	572	CloudHashing.com	Old/Historic	—
269	0000015549	565	565	Eligius.st	Pools	—
270	0000016775	527	527	Europex.eu	Old/Historic	—
271	0000017189	515	515	EveryDice.com	Old/Historic	—
272	0000018179	499	499	Brawker.com	Old/Historic	—
273	0000019489	473	471	10xBitco.in	Old/Historic	—
274	0000021056	440	1	Cubits.com	Services/Others	—
275	0000021084	440	439	BitMinter.com	Pools	—
276	0000021286	436	436	ExchangeMyCoins.com	Exchanges	Denmark
277	0000023185	402	402	BW.com	Pools	—
278	0000023304	400	400	Chainroll.com	Old/Historic	—
279	0000024708	390	390	DiceCoin.io	Gambling	—
280	0000025249	382	382	FoxBit.com.br	Exchanges	Brazil
281	0000025389	380	380	PonziCoin.co	Old/Historic	—
282	0000025554	377	377	Birwo.com-old	Old/Historic	—
283	0000027509	351	338	Zyado.com	Exchanges	Portugal
284	0000028306	341	341	SuzukiDice.com	Old/Historic	—
285	0000028897	334	1	Cubits.com	Services/Others	—
286	0000032828	297	297	KnCMiner.com	Pools	—
287	0000033285	293	293	BitcoinPokerTables.com	Gambling	—
288	0000034753	280	280	Polmine.pl	Old/Historic	—
289	0000034912	279	279	MineField.BitcoinLab.org	Gambling	—
290	0000045961	234	234	SmenarnaBitcoin.cz	Old/Historic	—
291	0000062902	195	195	Dgex.com	Old/Historic	—
292	0000064830	190	190	BitLauder.com	Services/Others	—
293	0000072390	170	170	BitMillions.com	Old/Historic	—
294	0000074148	166	1	Cubits.com	Services/Others	—
295	0000078381	157	1	Cubits.com	Services/Others	—
296	0000100904	125	125	Vic-Socks.to	Services/Others	—
297	0000108438	117	117	Gatecoin.com	Exchanges	China
298	0000109665	116	1	VirWoX.com	Exchanges	Austria
299	0000114095	112	112	Bitcoin-24.com	Old/Historic	—
300	0000157019	96	1	Cubits.com	Services/Others	—
301	0000180141	85	1	Poloniex.com	Exchanges	USA
302	0000200218	77	77	BetcoinDice.tm	Old/Historic	—
303	0000206094	75	75	Bitfury.org	Pools	—
304	0000265341	59	1	Cubits.com	Services/Others	—
305	0000296609	53	53	50BTC.com	Old/Historic	—
306	0000302266	52	1	Cubits.com	Services/Others	—
307	0000302626	52	1	Cubits.com	Services/Others	—
308	0000332619	49	49	BtcEur.eu	Old/Historic	—
309	0000417570	40	1	VirWoX.com	Exchanges	Austria
310	0000434094	38	1	Luno.com	Exchanges	South Africa
311	0000482184	35	35	SecureVPN.to	Services/Others	—
312	0000489034	34	1	Xapo.com	Services/Others	—
313	0000539744	32	32	MinersCenter.com	Old/Historic	—

Continue to next page

Table A-3 continued from previous page

No.	User ID	#Addr. (1)	#Addr. (2)	Name	Category	Country
314	0000661573	28	28	DiceOnCrack.com	Old/Historic	—
315	0000727720	26	1	Cubits.com	Services/Others	—
316	0000881383	23	1	Bittrex.com	Exchanges	USA
317	0001047894	20	20	ActionCrypto.com	Old/Historic	—
318	0001068642	20	1	Cubits.com	Services/Others	—
319	0001453639	15	1	CoinMotion.com	Exchanges	Finland
320	0001482058	15	15	ASICMiner	Old/Historic	—
321	0001615111	14	14	Telco214	Pools	—
322	0001849904	12	12	BTradeAustralia.com	Exchanges	Australia
323	0001949672	12	12	PinballCoin.com	Old/Historic	—
324	0002236961	11	1	MoonBit.co.in	Services/Others	—
325	0002437346	10	1	Cubits.com	Services/Others	—
326	0002652760	9	1	Xapo.com	Services/Others	—
327	0002867200	9	1	Cubits.com	Services/Others	—
328	0003042379	8	1	Xapo.com	Services/Others	—
329	0003656659	7	1	Cubits.com	Services/Others	—
330	0003733569	7	1	Luno.com	Exchanges	South Africa
331	0004053833	7	7	SimpleCoin.cz	Exchanges	Czech
332	0004615543	6	6	LuckyB.it	Gambling	—
333	0004719731	6	1	Cubits.com	Services/Others	—
334	0005083698	6	1	Cubits.com	Services/Others	—
335	0005134566	6	1	Cubits.com	Services/Others	—
336	0005316858	6	1	LakeBTC.com	Exchanges	China
337	0006291300	5	1	Cryptopay.me	Services/Others	—
338	0006553479	5	1	Xapo.com	Services/Others	—
339	0006787887	5	1	Cubits.com	Services/Others	—
340	0006884235	5	5	Exchanging.ir	Exchanges	Iran
341	0007872688	4	1	Cubits.com	Services/Others	—
342	0008064964	4	4	FoxBit.com.br	Exchanges	Brazil
343	0008251183	4	1	Cubits.com	Services/Others	—
344	0009938959	4	1	Cubits.com	Services/Others	—
345	0010541278	4	1	Bitcoin.de	Exchanges	Germany
346	0010933272	4	4	ePay.info	Services/Others	—
347	0011084834	4	1	Cubits.com	Services/Others	—
348	0011993584	3	1	Cubits.com	Services/Others	—
349	0013456456	3	3	EclipseMC.com	Pools	—
350	0014115232	3	1	Xapo.com	Services/Others	—
351	0014366385	3	1	Cubits.com	Services/Others	—
352	0014572029	3	1	StrongCoin.com-fee	Services/Others	—
353	0015020521	3	1	Poloniex.com	Exchanges	USA
354	0015254424	3	1	Cubits.com	Services/Others	—
355	0017326362	3	1	Cubits.com	Services/Others	—
356	0018289896	3	1	Huobi.com	Exchanges	China
357	0018738066	3	1	Cubits.com	Services/Others	—
358	0020356858	3	1	Poloniex.com	Exchanges	USA
359	0021062591	3	1	Cubits.com	Services/Others	—
360	0021163228	3	3	ePay.info	Services/Others	—
361	0021447975	2	1	Cubits.com	Services/Others	—
362	0022923752	2	1	Cubits.com	Services/Others	—
363	0023037394	2	1	Cubits.com	Services/Others	—
364	0024428379	2	1	Cubits.com	Services/Others	—
365	0026028525	2	1	Cubits.com	Services/Others	—
366	0033718608	2	1	Xapo.com	Services/Others	—
367	0034424835	2	1	VirWoX.com	Exchanges	Austria
368	0034774492	2	1	Cubits.com	Services/Others	—
369	0035023024	2	1	MercadoBitcoin.com.br	Exchanges	Brazil
370	0035093871	2	1	Huobi.com	Exchanges	China
371	0036244970	2	1	Cubits.com	Services/Others	—
372	0036353675	2	1	Cubits.com	Services/Others	—
373	0036389109	2	2	Dispenser.tf	Old/Historic	—
374	0039716556	2	1	Poloniex.com	Exchanges	USA
375	0040013060	2	1	Cubits.com	Services/Others	—
376	0045999467	2	2	DeepBit.net	Old/Historic	—
377	0046840841	2	1	Cubits.com	Services/Others	—

Continue to next page



*Table A-3 continued from previous page*

No.	User ID	#Addr. (1)	#Addr. (2)	Name	Category	Country
378	0047562289	2	1	Cubits.com	Services/Others	—
379	0049075064	2	1	Cubits.com	Services/Others	—
380	0050709449	2	1	Poloniex.com	Exchanges	USA
381	0051958689	2	2	CoinWorker.com	Services/Others	—
382	0052140982	2	1	Cubits.com	Services/Others	—
383	0053961615	2	1	Cubits.com	Services/Others	—
384	0055586746	2	1	Cubits.com	Services/Others	—
385	0056053704	2	1	Luno.com	Exchanges	South Africa
386	0058665155	2	1	Xapo.com	Services/Others	—
387	0058696998	2	1	Cubits.com	Services/Others	—
388	0058767317	2	1	Cubits.com	Services/Others	—
389	0059011161	2	1	Bittrex.com	Exchanges	USA

*End of Table A-3*

## Appendix B: Illustrating Adjacent Matrices of $G_t$ or $X_{sd}$

Fig. B-1 illustrates the adjacency matrices for all the networks  $G_t$  in Table I, or equivalently the non-negative matrix  $X_{sd}$  given by (15).

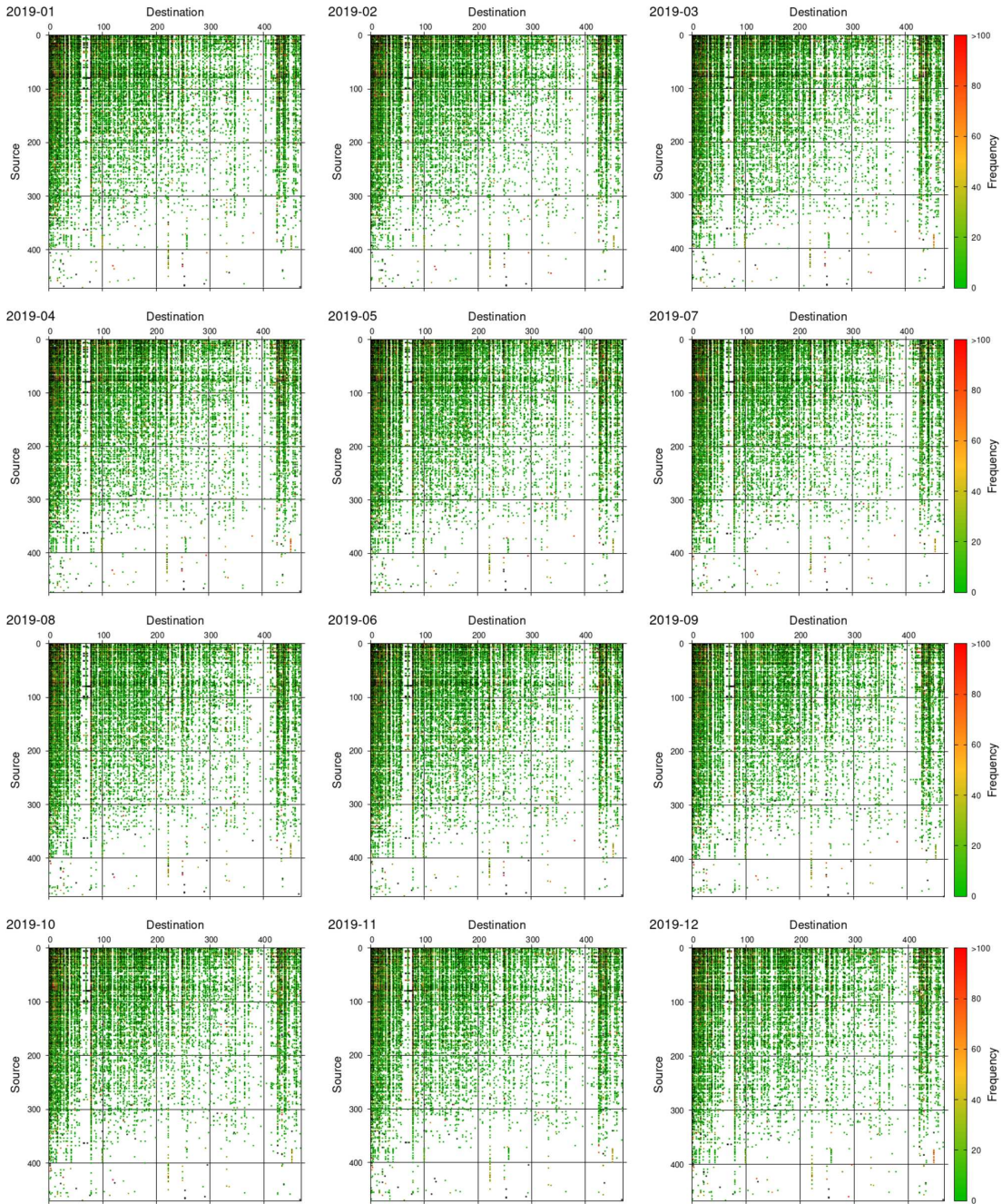


**Fig. B-1.** Adjacent matrices for all the networks  $G_t$  in Table I, or equivalently  $X_{sd}$  given by (15). Colors show the strength of links, expressed by the frequencies.

## Appendix C: Topic Model of Latent Dirichlet Allocation (LDA)

Topic models in natural language processing and machine learning are probabilistic models for how terms appear in documents in a given corpus. Assumed is the term frequency, irrespective of the sequential order of term occurrences; such an assumption is often called “bag-of-words”. A topic is a latent variable in the model for explaining term frequency occurrences. Latent Dirichlet allocation (LDA) [41] is such a model widely used in a variety of applications. See [37, 42, 43] and references therein for introduction and applications. In this appendix, we briefly summarize the topic model only for the purpose of explicitly relating it with non-negative matrix factorization (NMF).

$D$  documents in a corpus (a collection of documents) are given with a vocabulary of  $V$  terms (different words). Document  $d$  ( $d = 1, \dots, D$ ) comprises  $N_d$  words, possibly with duplication, each denoted by  $w_{dn}$  ( $n = 1, \dots, N_d$ ).  $K$  topics are assumed to be present for the given corpus. A topic is a latent or hidden variable giving a probability distribution for term occurrences. If a document is an article on sports, terms like “swimming” and “gymnastics” are likely to occur, while “market” and “employee” will be unlikely.

Consider the example of an article on “influence of hosting Olymics to economy” in a corpus of newspaper. It would be natural to consider that the article belongs to two topics of sports and economy. In topic models, documents are not assumed to belong to a single topic, but to simultaneously belong to multiple topics, and the topics vary among documents. Topic models aim at modeling such mixed membership.

Document  $d$  has a *topic distribution*, which is a multinomial distribution with the parameters:

$$\boldsymbol{\theta}_d = (\theta_{d1}, \dots, \theta_{dK}), \quad (\text{C}\cdot 1)$$

where  $\theta_{dk} = p(k | \boldsymbol{\theta}_d)$  is the probability that a topic  $k$  is assigned to the document  $d$ , satisfying

$$\theta_{dk} \geq 0 \quad \text{and} \quad \sum_{k=1}^K \theta_{dk} = 1. \quad (\text{C}\cdot 2)$$

Then a topic  $z_{dn} \in \{1, \dots, K\}$  is assigned to each word  $w_{dn}$  for  $n = 1, \dots, N_d$ . Each topic  $k$  is a *term distribution*, which is also a multinomial distribution with the parameters:

$$\boldsymbol{\phi}_k = (\phi_{k1}, \dots, \phi_{kV}), \quad (\text{C}\cdot 3)$$

where  $\phi_{kv} = p(v | \boldsymbol{\phi}_k)$  is the probability that a term  $v$  occurs, satisfying

$$\phi_{kv} \geq 0 \quad \text{and} \quad \sum_{v=1}^V \phi_{kv} = 1. \quad (\text{C}\cdot 4)$$

The topic model of LDA can be most readily understood by looking at how it generates words in documents as follows.

1. For each topic  $k = 1, \dots, K$ , generate the parameters  $\boldsymbol{\phi}_k$  for the term distribution by

$$\boldsymbol{\phi}_k \sim \text{Dir}(\boldsymbol{\beta}), \quad (\text{C}\cdot 5)$$

where  $\sim$  reads that a variable is realized as a sample from the distribution on the right-hand side, and  $\text{Dir}(\cdot)$  is the Dirichlet distribution<sup>7</sup>.  $\boldsymbol{\beta} = (\beta_1, \dots, \beta_V)$  is a set of hyper-parameters with  $\beta_i > 0$ .

---

<sup>7</sup>Dirichlet distribution is defined by

$$\text{Dir}(\mathbf{x} | \boldsymbol{\xi}) = \frac{\Gamma(\sum_{i=1}^I \xi_i)}{\prod_{i=1}^I \Gamma(\xi_i)} \times \prod_{i=1}^I x_i^{\xi_i - 1},$$

where  $I$  is the number of variables and it is assumed that  $x_i \geq 0$  for all  $i$  and  $\sum_{i=1}^I x_i = 1$ .  $\Gamma(\cdot)$  is the gamma function defined by  $\Gamma(u) = \int_0^\infty t^{u-1} e^{-t} dt$  for  $u > 0$ . Dirichlet distribution is a generalization of Beta distribution (the case  $I = 2$ ).

2. Now for each document  $d = 1, \dots, D$ ,

(a) generate the parameters  $\theta_d$  for the topic distribution by

$$\theta_d \sim \text{Dir}(\alpha), \quad (\text{C-6})$$

where  $\alpha = (\alpha_1, \dots, \alpha_K)$  is a set of hyper-parameters with  $\alpha_k > 0$ .

(b) For each word  $w_{dn}$  ( $n = 1, \dots, N_d$ )

(i) generate a topic by

$$z_{dn} \sim \text{Cat}(\theta_d), \quad (\text{C-7})$$

where  $\text{Cat}(\cdot)$  is the categorical distribution<sup>8</sup>, and then

(ii) generate a word from the vocabulary by

$$w_{dn} \sim \text{Cat}(\phi_{k=z_{dn}}). \quad (\text{C-8})$$

Note that a topic is assigned to each occurrence of word  $w_{dn}$  at the location  $n$  of the document  $d$ , depending on how the document  $d$  has a mixture of topics, but is not associated with each term  $v$  in the vocabulary of  $V$  terms. In the previous example, the term “swimming” occurs with a relatively high probability if the topic of sports is assigned at the location of occurrence, but the term will not be likely to occur if the topic of economy is assigned at the same location.

Given the number of topics,  $K$ , and the hyper-parameters,  $\beta$  and  $\alpha$ , the model  $\mathcal{M}$  can be specified by the parameters  $\{\theta_d\}_{d=1, \dots, D}$  and  $\{\phi_k\}_{k=1, \dots, K}$ , while the data  $\mathcal{D}$  comprises  $D$  documents, each of which is a set of words  $\{w_{dn}\}_{n=1, \dots, N_d}$  for  $d = 1, \dots, D$ . In the Bayesian framework of

$$p(\mathcal{M} | \mathcal{D}) = \frac{p(\mathcal{D} | \mathcal{M}) \cdot p(\mathcal{M})}{p(\mathcal{D})}. \quad (\text{C-9})$$

the prior distribution  $p(\mathcal{M})$  is given by the Dirichlet distributions of (C-5) and (C-6). It is easy to show that the likelihood  $p(\mathcal{D} | \mathcal{M})$  can be written by

$$\log p(\mathcal{D} | \mathcal{M}) = \sum_{d=1}^D \sum_{n=1}^{N_d} \log \sum_{k=1}^K \theta_{dk} \cdot \phi_{kw_{dn}}, \quad (\text{C-10})$$

which follows from the assumption of bag-of-words and the independence of documents. Estimation of parameters by maximum likelihood or Bayesian frameworks has a difficulty due to the log of sum in (C-10), so there are a variety of technical methods such as EM (expectation and maximization), variational Bayes, and MCMC (Markov chain Monte Carlo) algorithms (see [37, 42, 43] and references therein).

For our purpose, let us turn our attention to how a word is chosen from the  $V$  terms in the vocabulary in the  $D$  documents, given the model parameters. Looking at (C-7) and (C-8), one can see that the probability that a term  $v$  is chosen as a word in the document  $d$ , denoted by  $\lambda_{dv}$ , is given by

$$\lambda_{dv} = \sum_{k=1}^K \theta_{dk} \cdot \phi_{kv}, \quad (\text{C-11})$$

where it is assumed that

$$\lambda_{dv} \geq 0 \quad \text{and} \quad \sum_{v=1}^V \lambda_{dv} = 1. \quad (\text{C-12})$$

---

<sup>8</sup>Categorical distribution is a multinomial distribution for a single trial (a roll of a dice), i.e.

$$\text{Cat}(v | \phi) = \phi_v,$$

where  $v \in \{1, \dots, V\}$  and  $\phi = (\phi_1, \dots, \phi_V)$  with  $\phi_v \geq 0$  for all  $v$  and  $\sum_v \phi_v = 1$ .

(Note that (C·11) is the factor in the likelihood (C·10)). In terms of matrices, the  $D \times V$  matrix, denoted by  $\mathbf{\Lambda}$ , with elements  $\lambda_{dv}$  is represented by a product of two matrices; the  $D \times K$  matrix  $\mathbf{\Theta}$  with elements  $\theta_{dk}$  times the  $K \times V$  matrix  $\mathbf{\Phi}$  with elements  $\phi_{kv}$ . Note that it is usually the case that  $K \ll V$  and  $K \ll D$ . One can immediately see that (C·11) is actually a non-negative matrix factorization (NMF) of  $\mathbf{\Lambda}$  by two generally much smaller matrices:

$$\mathbf{\Lambda} = \mathbf{\Theta} \cdot \mathbf{\Phi} \tag{C·13}$$

under the conditions of (C·2) and (C·4), from which (C·12) follows.

A document-term matrix is the  $D \times V$  matrix, the rows and columns of which correspond to the documents and terms respectively, and each element is the frequency (or any other measure that represents some intensity) for the term occurrences. One can regard the document-term matrix as a realization in the sense that each element at column  $v$  and row  $d$  represents how the term  $v$  was realized in the document  $d$  according to the categorical (multinomial) distribution with the parameter  $\lambda_{dv}$ . See the main text in Section 3.4.

How to determine the number of topics,  $K$ , is important. There have been a number of works on this issue. A class of studies [38–40] is based on some measure to compute similarities of extracted topics, called coherence. The idea is that an optimal value of  $K$  is the point where the overall dissimilarity among topics achieves a maximum, because extracted topics should be different to a certain degree. Other approaches include the idea of perplexity [37], hierarchical Dirichlet process [44], and so forth. It is beyond the present paper to review these approaches. Interested readers are guided to look at them and reviews [42, 43] with references therein. In the main text, we use the idea of coherence [38–40], which we find to work well for our purpose.

### Appendix D: Optimal Number of NMF Components

In Section 3.4, we showed that the matrix decomposition of NMF can be regarded as a probabilistic model, which is equivalent to a model of probabilistic latent semantic analysis (PLSA) in natural language processing, in particular, latent Dirichlet allocation (LDA). The number of NMF components is such an analogous parameter as the number of topics in the latter. Then, as a bonus, one can employ the method of estimating the number of topics to our problem of determining the number of NMF components,  $K$ . We found that three different methods in the literature [38–40] give a consistent result for the optimal value of  $K$ , and also that one of them [39] is relatively stable in giving the optimal (see Fig. 8).

In Fig. D-1, we summarize the same result for the data in all the other months in the same year. We found that the optimal number  $K$  is not volatile in its variation among different months, and also small in its value ranging around 11–18. Table D-1 shows the optimal values for all the months of the year 2019.

**Table D-1.** Optimal values for the number of NMF components,  $K$ , estimated from Fig. D-1

Month	Optimal $K$
01	14
02	16
03	18
04	16
05	16
06	18
07	15
08	12
09	13
10	11
11	13
12	13

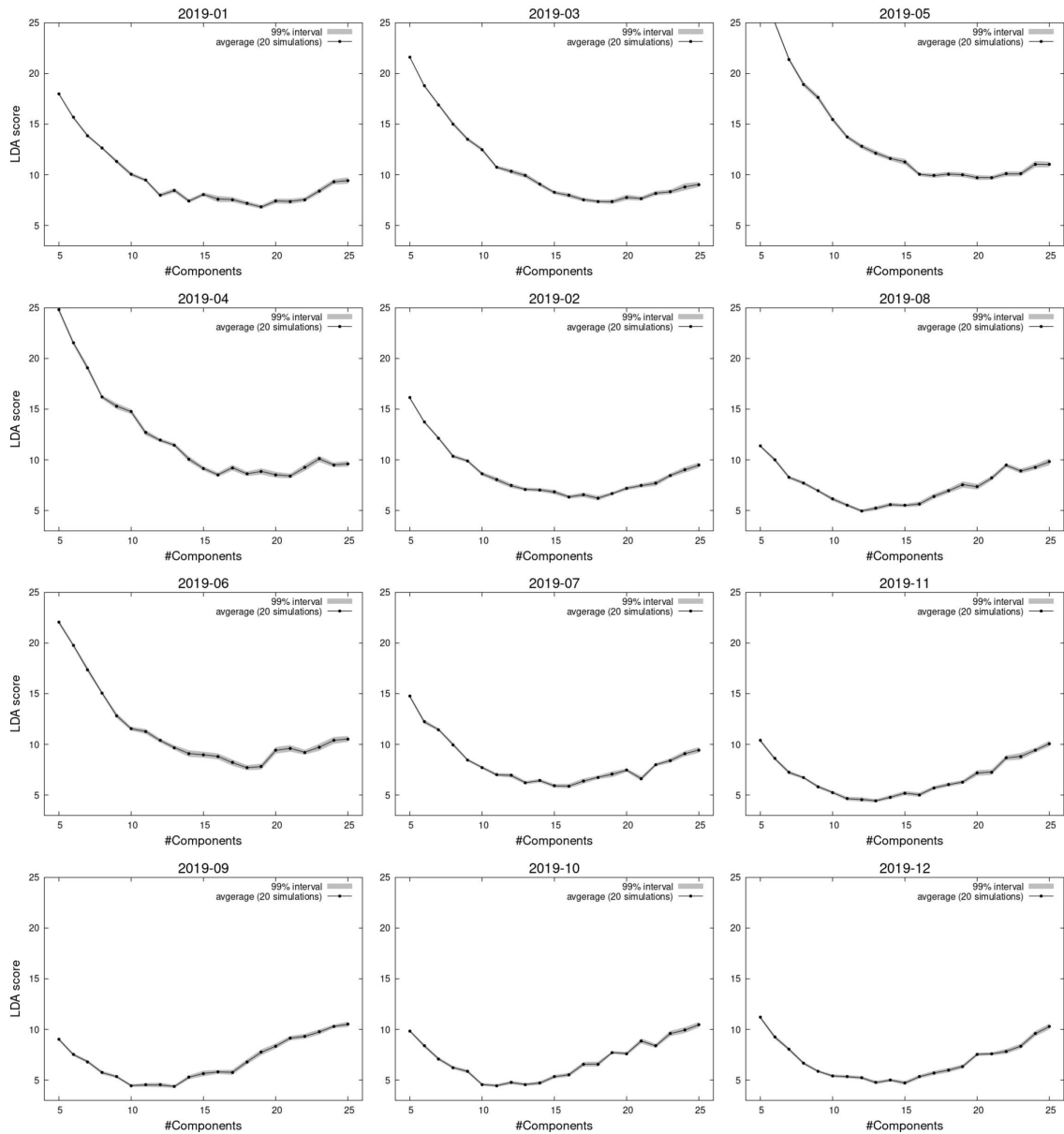


**Fig. D-1.** Determining  $K$ , the number of NMF components, by minimizing the measure of coherence [39]. We performed Monte Carlo simulations with 20 runs for each number of components. Averages (points) and 99% level (gray band, narrow) calculated from standard errors are drawn. Data: all months in the year 2019.